

Electronic Supporting Information (ESI)

**Photocatalytic glucose-appended bio-compatible Ir(III) anticancer complexes**

Zilin Zhu,<sup>a</sup> Li Wei,<sup>a</sup> Yidan Lai,<sup>b</sup> Oliver W. L. Carter,<sup>c</sup> Samya Banerjee,<sup>d</sup> Peter J. Sadler\*<sup>c</sup> and  
Huaiyi Huang\*<sup>a</sup>

<sup>a</sup>*School of Pharmaceutical Sciences (Shenzhen), Shenzhen Campus of Sun Yat-sen University, Sun Yat-sen University, Shenzhen 518107, P. R. China. E-mail: [huanghy87@mail.sysu.edu.cn](mailto:huanghy87@mail.sysu.edu.cn)*

<sup>b</sup>*College of Chemistry and Environmental Engineering, Shenzhen University, Shenzhen, 518060, P. R. China.*

<sup>c</sup>*Department of Chemistry, University of Warwick, Coventry CV4 7AL, UK. E-mail: [P.J.Sadler@warwick.ac.uk](mailto:P.J.Sadler@warwick.ac.uk)*

<sup>d</sup>*Department of Chemistry, Indian Institute of Technology (BHU), Varanasi, UP-221005, India.*

## Contents

### Experimental section

#### Tables

**Table S1.** Solubility of **Ir1-Ir4** in H<sub>2</sub>O at 25 °C

**Table S2.** Fluorescence quantum yields ( $\Phi$ ) of **Ir1-Ir3**

**Table S3.** Log P<sub>o/w</sub> values of **Ir1-Ir4**

**Table S4.** Singlet oxygen generation quantum yield ( $\Phi_{\Delta}$ ) of **Ir1-Ir3**

**Table S5.** TONs and TOFs of **Ir1-Ir3** for NADH /NADPH photo-oxidation

**Table S6.** Photo- and dark-cytotoxicity of **Ir1-Ir3** against A549 and B16 cells after 465 nm blue light irradiation.

#### Figures

**Fig. S1.** <sup>1</sup>H NMR and <sup>1</sup>H-<sup>1</sup>H 2D COSY NMR spectrum of GlcOAc ligand

**Fig. S2.** <sup>1</sup>H NMR and <sup>1</sup>H-<sup>1</sup>H 2D COSY NMR spectrum of GlcOH ligand

**Fig. S3.** <sup>1</sup>H NMR and <sup>1</sup>H-<sup>1</sup>H 2D COSY NMR spectrum of **Ir1**

**Fig. S4.** <sup>13</sup>C NMR spectrum of **Ir1**

**Fig. S5.** ESI-MS, HRMS spectrum and HPLC chromatogram of **Ir1**

**Fig. S6.** <sup>1</sup>H NMR and <sup>1</sup>H-<sup>1</sup>H 2D COSY NMR spectrum of **Ir2**

**Fig. S7.** <sup>13</sup>C NMR spectrum of **Ir2**

**Fig. S8.** ESI-MS, HRMS spectrum and HPLC chromatogram of **Ir2**

**Fig. S9.** <sup>1</sup>H NMR and <sup>1</sup>H-<sup>1</sup>H 2D COSY NMR spectrum of **Ir3**

**Fig. S10.** <sup>13</sup>C NMR spectrum of **Ir3**

**Fig. S11.** ESI-MS, HRMS spectrum and HPLC chromatogram of **Ir3**

**Fig. S12.** <sup>1</sup>H NMR and ESI-MS spectrum of **Ir4**

**Fig. S13.** UV-vis and phosphorescence spectra of **Ir1-Ir3**

**Fig. S14.** Phosphorescence spectra of **Ir1-Ir3** in air or nitrogen-saturated H<sub>2</sub>O and CH<sub>2</sub>Cl<sub>2</sub>

**Fig. S15.** UV-vis spectra to determine the dark and light stability of **Ir1-Ir3**

**Fig. S16.** Determination of singlet oxygen generation of **Ir1-Ir3** by ABDA

**Fig. S17.** The slopes of plots of the absorbance of ABDA vs. the irradiation times in the presence of **Ir1-Ir3**

**Fig. S18.** Determination of singlet oxygen generation by **Ir3** under 525 nm green light

**Fig. S19.** Photocatalytic oxidation of NADH/NADPH by **Ir1-Ir3** and detection of H<sub>2</sub>O<sub>2</sub> production during the photo-oxidation

**Fig. S20.** Turnover numbers (TON) and turnover frequency (TOF) calculations from spectra of **Ir1-Ir3** for NADH /NADPH photo-oxidation

**Fig. S21.** Detection of H<sub>2</sub>O<sub>2</sub> in PBS solution produced by **Ir1-Ir3**

**Fig. S22.** Time-dependent cellular uptake of **Ir2** and **Ir3** using flow cytometry

**Fig. S23.** Confocal images of HeLa cells, incubated with **Ir1-Ir3** and various commercial organelle trackers

**Fig. S24.** Intracellular generation of singlet oxygen ( $^1\text{O}_2$ ) in HeLa cells, induced by **Ir1-Ir3** on light irradiation

**Fig. S25.** Intracellular generation of superoxide radicals ( $\text{O}_2^{\cdot-}$ ) in HeLa cells, induced by **Ir1-Ir3** on light irradiation

**Fig. S26.** Change in the mitochondrial membrane potential in HeLa cells by **Ir1-Ir3** on light irradiation

**Fig. S27.** Photo-induced necro-apoptotic death of HeLa cells by **Ir1-Ir3** from Annexin V/PI staining

**Fig. S28.** Photo-induced necro-apoptotic death of HeLa cells by **Ir3** using flow cytometry

**Fig. S29.** Z-stack scanning of MCTSs after incubation with **Ir3**

**Fig. S30.** Long-term MCTSs growth inhibition by **Ir3** on light irradiation

**Fig. S31.** Effect of **Ir3** on development and survival of zebrafish embryos and larvae

**References**

## Experimental section

### Materials

$\text{IrCl}_3 \cdot 3\text{H}_2\text{O}$  and acetobromo- $\alpha$ -D-glucose were purchased from Aladdin. 2-ethynylpyridine, 2-phenylpyridine, coumarin 6, 2,2'-bipyridine and 9,10-anthracenediyl-bis(methylene)dimalonic acid (ABDA) were purchased from Bidepharm, 1-phenylisoquinoline,  $\text{CuSO}_4 \cdot 5\text{H}_2\text{O}$  and sodium methylate from Macklin, and  $\text{Na}_2\text{CO}_3$  from Damao Chemical Reagent Factory. AG<sup>®</sup> 50W-X8 resin was purchased from Bio-Rad Laboratories, Inc.  $\beta$ -Nicotinamide adenine dinucleotide, reduced disodium salt I ( $\beta$ -NADH) and  $\beta$ -Nicotinamide adenine dinucleotide phosphate, reduced disodium salt II ( $\beta$ -NADPH) from Sigma-Aldrich, and 3-(4,5-dimethylthiazol-2-yl)-2,5-diphenyltetrazolium bromide (MTT) from Macklin. Human cervical cancer cell line (HeLa) and human lung carcinoma cell line (A549) were obtained from Sun Yat-Sen University (Guangzhou, China). Murine melanoma cell line (B16) was purchased from Shanghai Qida Biotechnology Co., Ltd. Dulbecco Modified Eagle Medium (DMEM), Roswell Park Memorial Institute medium (RPMI-1640), fetal bovine serum (FBS), penicillin/streptomycin were obtained from Gibco. Mito Tracker<sup>®</sup>Red, Lyso Tracker<sup>®</sup>Deep Red and JC-1 were purchased from Life Technologies Corporation. Oxygen Sensor Green Reagent (SOSG) was purchased from Dalian Meilun Biotechnology. Dihydroethidium (DHE) and Annexin V-FITC/PI Apoptosis Detection Kit were purchased from Beyotime Biotechnology.

### Instruments

$^1\text{H}$  NMR,  $^1\text{H}$ - $^1\text{H}$  2D COSY and  $^{13}\text{C}$  NMR spectra were recorded on a Bruker AV-400 or AV-600 spectrometers. Positive ion electrospray ionization mass spectra (ESI-MS) were obtained on a Thermo LTQ XL Ion Trap LC-MS. High Resolution mass spectra were recorded by LCMS-IT-TOF (Shimadzu, Japan) instrument. HPLC spectra were analyzed by LC-20 AT HPLC system (Shimadzu, Japan). UV-vis spectra were recorded on a PerkinElmer Lambda 600 UV-vis spectrophotometer. Emission spectra and the emission quantum yield measurements were made using a Techcomp FL970 fluorescence spectrophotometer. Confocal microscopy visualized by laser confocal microscopy (LSM 880, Carl Zeiss, Göttingen, Germany). Visible irradiation ( $\lambda_{\text{irr}} = 465 \pm 5$  nm, 65 mW/cm<sup>2</sup>, 100% power) for PDT was provided by a commercially available LED visible area light source (Height LED Instruments, China). Green light irradiation ( $\lambda_{\text{irr}} = 525$  nm, range of 460-655 nm) was done by a commercially available LED visible light source (Puri Materials, China).

### Synthesis

#### *Synthesis of GlcOAc ligand*

To a mixture of ascorbic acid (0.176 g, 1.0 mmol),  $\text{CuSO}_4 \cdot 5\text{H}_2\text{O}$  (0.049 g, 0.2 mmol) and  $\text{Na}_2\text{CO}_3$  (0.317 g, 3 mmol) in  $\text{H}_2\text{O}$  (10 mL), a mixture of 2-ethynylpyridine (0.103 g, 1 mmol), sodium azide (0.078 g, 1.2 mmol) and acetobromo- $\alpha$ -D-glucose (0.452 g, 1.1 mmol) in DMF (12 mL) was added.

The resultant reaction mixture was stirred at room temperature for 24 h. EDTA/NH<sub>3</sub>·H<sub>2</sub>O (50mL) solution was then added and stirred at room temperature for another 1 h. A significant amount of white precipitate formed during stirring. The precipitate was then filtered off, washed with water and finally dried in vacuum to obtain a white solid. Yield: 0.252 g, 86.8%. <sup>1</sup>H NMR (400 MHz, chloroform-*d*) δ 8.63 (d, *J* = 4.8 Hz, 1H), 8.43 (s, 1H), 8.17 (d, *J* = 7.9 Hz, 1H), 7.81 (td, *J* = 7.8, 1.7 Hz, 1H), 7.28-7.23 (m, 1H), 5.95 (d, *J* = 8.8 Hz, 1H), 5.57-5.43 (m, 2H), 5.29 (t, *J* = 9.5 Hz, 1H), 4.34 (dd, *J* = 12.6, 4.8 Hz, 1H), 4.19 (dd, *J* = 12.6, 1.9 Hz, 1H), 4.05 (ddd, *J* = 10.1, 4.8, 2.0 Hz, 1H), 2.12(s, 3H), 2.10 (s, 3H), 2.07 (s, 3H), 1.92 (s, 3H).

#### ***Synthesis of GlcOH ligand***

Purified GlcOAc ligand (0.477 g, 1.0 mmol) in MeOH (10 mL), sodium methylate (1 mL, 0.1 M in MeOH) was added and then the mixture was stirred at room temperature for 3 h. The solution was then neutralized with AG<sup>®</sup> 50W-X8 resin and filtered. The solvents were evaporated under vacuum to give the pure GlcOH ligand. Yield: 0.230 g, 74.6%. <sup>1</sup>H NMR (400 MHz, methanol-*d*<sub>4</sub>) δ 8.66(s, 1H), 8.61 (br, 1H), 8.12 (d, *J* = 7.4 Hz, 1H), 8.02-7.91 (m, 1H), 7.54-7.31 (m, 1H), 5.72 (d, *J* = 9.2 Hz, 1H), 3.99 (t, *J* = 9.0 Hz, 1H), 3.93 (dd, *J* = 12.2, 1.9 Hz, 1H), 3.77 (dd, *J* = 12.2, 5.4 Hz, 1H), 3.70-3.52 (m, 3H).

#### ***Synthesis of μ-dichloro bridged Ir(III) dimer complexes***

A mixture of IrCl<sub>3</sub>·3H<sub>2</sub>O (0.358 g, 1.0 mmol) and the corresponding ligand (2.24 mmol) in 2-ethoxyethanol/water (16 mL, v/v=3/1) was refluxed with continuous stirring at 110 °C for 24 h. Then the solution was cooled to room temperature and filtered. Next, the residue was dried to give the desired powder and was directly used in the following reactions without further purification.

#### ***Synthesis of complexes Ir1-Ir4***

The respective μ-dichloro bridged Ir(III) dimer (0.125 mmol) and GlcOAc, GlcOH or 2,2'-bipyridine ligand (0.250 mmol) were suspended in CHCl<sub>3</sub>/MeOH (15 mL, v/v=2/1). The mixture was heated for 24 h at 60 °C with continuous stirring. The solvent was removed under vacuum. The crude product was purified by column chromatography on neutral alumina. After this, the preparation of **Ir1** and **Ir2** complexes required the experimental step of deacetylation. **Ir4** was synthesized according to previous literature.<sup>[1]</sup>

**Complex Ir1:** The complex was obtained as a yellow powder by a step of the Ir(III) dimer with 2-phenylpyridine (0.348 g, 2.24 mmol) and GlcOAc, followed by deacetylation. The crude product was purified by column chromatography on neutral alumina, and then the product was dissolved in methanol, sodium methylate was added (for deacetylation), and stirred at room temperature for 3 h. The solution was then neutralized with AG<sup>®</sup> 50W-X8 resin and filtered. The solvents were evaporated under vacuum to give the pure **Ir1** complex. Yield: 0.051 g, 47.9%. ESI-MS, *m/z* (%):809.20 (100), [M-Cl]<sup>+</sup>. HRMS-MS (*m/z*): expected 809.2060 [M-Cl]<sup>+</sup>, found 809.2061

[M-Cl]<sup>+</sup>. <sup>1</sup>H NMR (400 MHz, methanol-*d*<sub>4</sub>) δ 9.43 (s, 0.5H), 9.40 (s, 0.5H), 8.31 (d, *J* = 7.9 Hz, 1H), 8.25-8.04 (m, 3H), 7.99-7.84 (m, 3H), 7.83 (d, *J* = 7.7 Hz, 1H), 7.80-7.70 (m, 2H), 7.67 (d, *J* = 5.7 Hz, 1H), 7.52-7.39 (m, 1H), 7.21-6.99 (m, 3H), 7.01-6.86 (m, 2H), 6.84-6.75 (m, 1H), 6.28 (q, *J* = 7.8, 7.4 Hz, 2H), 5.79-5.69 (m, 1H), 3.93-3.45 (m, 6H). <sup>13</sup>C NMR (150 MHz, methanol-*d*<sub>4</sub>) δ 169.89, 169.19, 169.14, 166.84, 151.60, 151.56, 150.80, 150.76, 150.75, 150.72, 150.50, 150.47, 150.16, 150.04, 150.00, 147.24, 145.44, 145.42, 145.38, 141.05, 139.70, 139.59, 139.56, 133.02, 133.01, 132.64, 132.57, 131.52, 130.71, 128.11, 128.08, 125.98, 125.48, 125.44, 124.50, 124.47, 124.19, 124.17, 123.99, 123.83, 123.25, 120.93, 120.86, 117.19, 90.81, 90.66, 81.64, 81.55, 81.55, 78.37, 78.17, 74.66, 73.88, 70.83, 70.76, 70.76, 62.25, 62.11, 49.59.

**Complex Ir2:** The complex was obtained as an orange powder by treatment of the Ir(III) dimer with 1-phenylisoquinoline (0.460 g, 2.24 mmol) and GlcOAc. The crude product was purified by column chromatography on neutral alumina, and then the product was dissolved in methanol, sodium methylate was added (for deacetylation), and stirred at room temperature for 3 h. The solution was then neutralized with AG® 50W-X8 resin and filtered. The solvents were evaporated under vacuum to give the pure **Ir2** complex. Yield: 0.052 g, 44.0%. ESI-MS, *m/z*(%):909.25 (100), [M-Cl]<sup>+</sup>. HRMS-MS (*m/z*): expected 909.2374 [M-Cl]<sup>+</sup>, found 909.2411 [M-Cl]<sup>+</sup>. <sup>1</sup>H NMR (400 MHz, methanol-*d*<sub>4</sub>) δ 9.45 (s, 0.5H), 9.42 (s, 0.5H), 9.09-9.01 (m, 2H), 8.37 (d, *J* = 8.1 Hz, 1H), 8.35-8.28 (m, 2H), 8.16-8.10 (m, 1H), 8.05-7.99 (m, 2H), 7.91-7.84 (m, 4H), 7.82 (d, *J* = 5.6 Hz, 1H), 7.62 (dd, *J* = 6.5, 2.5 Hz, 1H), 7.57 (dd, *J* = 6.4, 2.8 Hz, 1H), 7.56-7.39 (m, 3H), 7.23-7.10 (m, 1H), 7.12-7.00 (m, 1H), 6.97-6.85 (m, 1H), 6.89-6.71 (m, 1H), 6.41-6.25 (m, 2H), 5.76-5.68 (m, 1H), 3.90-3.47 (m, 6H). <sup>13</sup>C NMR (100 MHz, DMSO-*d*<sub>6</sub>) δ 168.43, 168.37, 167.97, 167.94, 153.49, 153.26, 150.36, 150.29, 149.96, 149.92, 149.23, 149.12, 149.07, 148.62, 145.75, 145.71, 145.68, 141.42, 141.11, 140.98, 140.70, 137.05, 137.02, 136.99, 132.57, 132.48, 132.35, 132.32, 131.79, 131.70, 131.00, 130.96, 130.62, 130.58, 130.20, 130.17, 129.94, 129.88, 129.82, 129.78, 128.23, 128.20, 128.18, 127.71, 126.90, 126.89, 126.81, 126.76, 126.00, 125.95, 123.56, 123.46, 122.94, 122.91, 122.87, 122.72, 122.65, 122.59, 122.33, 122.28, 89.44, 89.17, 80.66, 80.37, 76.76, 76.22, 73.67, 72.94, 72.22, 69.83, 69.74, 65.94, 63.26, 60.91, 60.75, 60.69.

**Complex Ir3:** The complex was obtained as an orange powder by reacting the Ir(III) dimer with coumarin 6 (0.784 g, 2.24 mmol) and GlcOH. Yield: 0.039 g, 25.0%. ESI-MS, *m/z*(%):1199 (100), [M-Cl]<sup>+</sup>. HRMS-MS (*m/z*): expected 1199.2767 [M-Cl]<sup>+</sup>, found 1199.2752 [M-Cl]<sup>+</sup>. <sup>1</sup>H NMR (400 MHz, methanol-*d*<sub>4</sub>) δ 9.32 (s, 0.55H), 9.26 (s, 0.45H), 8.90-8.78 (m, 1H), 8.23-8.15 (m, 1H), 8.10-8.03 (m, 1H), 8.02-7.96 (m, 1H), 7.93 (dd, *J* = 7.7, 3.3 Hz, 1H), 7.82-7.72 (m, 1H), 7.32-7.21 (m, 2H), 7.22-7.11 (m, 1H), 7.03-6.94 (m, 1H), 6.46-6.34 (m, 2H), 6.31-6.11 (m, 4H), 6.08-5.98 (m, 2H), 5.97-5.83 (m, 1H), 3.94-3.45 (m, 6H), 3.33-3.22 (m, 8H), 1.21-0.84 (m, 12H). <sup>13</sup>C NMR (100 MHz, methanol-*d*<sub>4</sub>) δ 178.18, 178.13, 177.35, 177.32, 177.19, 177.16, 158.28, 157.93, 157.12, 155.12, 154.68, 152.93, 152.91, 152.67, 150.55, 149.21, 149.19, 148.85, 148.81, 147.96, 147.91, 147.70, 147.64, 141.44, 132.25, 132.20, 131.91, 131.49, 131.40, 131.09, 131.01, 128.19, 127.82, 127.76, 127.00, 126.93, 125.76, 124.59, 124.49, 124.43, 124.33, 123.41, 123.39, 123.08, 122.97,

122.69, 122.64, 122.31, 122.20, 121.46, 118.82, 118.79, 118.67, 118.65, 116.40, 116.10, 115.95, 115.88, 109.61, 109.45, 96.18, 96.02, 95.98, 89.73, 89.49, 80.27, 80.14, 76.94, 76.78, 73.94, 71.98, 69.49, 69.32, 61.02, 60.58, 44.29, 44.24, 11.31, 11.28.

**Complex Ir4:** The complex was obtained as an orange powder by reacting the Ir(III) dimer with coumarin 6 (0.784 g, 2.24 mmol) and 2,2'-bipyridine. Yield: 0.073 g, 54.0%. ESI-MS, m/z(%):1047 (100), [M-Cl]<sup>+</sup>. <sup>1</sup>H NMR (400 MHz, chloroform-*d*) δ 8.59 (d, *J* = 8.2 Hz, 2H), 8.57-8.50 (m, 2H), 8.27 (td, *J* = 8.0, 1.6 Hz, 2H), 7.88-7.80 (m, 2H), 7.71-7.63 (m, 2H), 7.34-7.29 (m, 1H), 7.28-7.23 (m, 1H), 7.01-6.93 (m, 2H), 6.40 (d, *J* = 2.7 Hz, 2H), 6.12-6.02 (m, 2H), 5.89 (dd, *J* = 9.5, 2.7 Hz, 2H), 5.82 (d, *J* = 8.5 Hz, 2H), 3.31 (q, *J* = 7.3 Hz, 8H), 1.12 (t, *J* = 7.1 Hz, 12H).

### HPLC analysis

The purity and retention time of complexes **Ir1-Ir3** were determined by analytical HPLC (LC-20 AT, Shimadzu, Japan) with a Agilent ZORBAX SB-C18 column. The runs were performed with a linear gradient of A phase (H<sub>2</sub>O:CH<sub>3</sub>CN:Formic acid, 950:50:1) and B phase (CH<sub>3</sub>CN:Formic acid, 1000:1): t = 0 min, 95 % A; t = 20 min, 100 % B. The mobile phase flow rate was 1 mL/min. The UV detection was set at 290 nm using a Diode Array Detector for **Ir1-Ir3**.

### UV-vis spectroscopy

The UV-vis spectra were obtained with a PerkinElmer Lambda 600 UV-vis spectrophotometer. The UV-vis spectra of **Ir1-Ir3** (10 μM) in a 1-cm quartz cuvette with eight different solvents were obtained at room temperature from 700 to 300 nm. The complexes (10 μM) in the different solvents were diluted from a stock solution in DMSO (10 mM).

### Phosphorescence spectra

Phosphorescence emission measurements were performed on a Techcomp FL970 fluorescence spectrophotometer. The complex **Ir1** (10 μM) in the different solvents were excited at λ<sub>ex</sub> = 405 nm in a 1 cm quartz cuvette at room temperature. Complexes **Ir2** (10 μM) and **Ir3** (10 μM) were excited at λ<sub>ex</sub> = 458 nm and 488 nm respectively.

### Emission quantum yield measurements

Emission spectra were obtained using a Techcomp FL970 fluorescence spectrophotometer. The relative emission quantum yields were determined with [Ru(bpy)<sub>3</sub>]Cl<sub>2</sub> as the standard by the following equation:

$$\Phi_x = \Phi_{\text{std}} * (F_x/F_{\text{std}}) * (A_{\text{std}}/A_x) * (n_x/n_{\text{std}})^2$$

where Φ represents quantum yield; F stands for integrated area under the corrected emission spectrum; A is absorbance at the excitation wavelength; n is the refractive index of the solution; and the subscripts x and std indicate the sample and standard [Ru(bpy)<sub>3</sub>]Cl<sub>2</sub>, respectively. Ir(III) complexes were diluted from a stock solution in DMSO (1 mM or 10 mM) to achieve an absorbance

= 0.1 at 465 nm in water or acetonitrile. The complexes were excited at  $\lambda_{ex} = 465$  nm at 298 K. The emission quantum yield ( $\Phi$ ) for  $[\text{Ru}(\text{bpy})_3]\text{Cl}_2$  were 0.040 in aerated  $\text{H}_2\text{O}$  and 0.018 in aerated  $\text{CH}_3\text{CN}$ . The emission quantum yield ( $\Phi$ ) for  $[\text{Ru}(\text{bpy})_3]\text{Cl}_2$  were 0.063 in deaerated  $\text{H}_2\text{O}$  and 0.095 in deaerated  $\text{CH}_3\text{CN}$ .<sup>[2]</sup>

### **Log $P_{o/w}$ measurement**

A pre-saturated water and n-octanol mixture was obtained by shaking the mixture of water and n-octanol for 24 h. Complexes **Ir1-Ir4** were added to 1 mL pre-saturated n-octanol and 1 mL pre-saturated water solution, and the final concentration of the complexes was 50  $\mu\text{M}$ , then the mixture was shaken overnight in the dark at room temperature. When stationary, the absorbance of complexes in the oil/water phase was determined by a microplate reader. The partition coefficient of the complex was calculated from the equation  $\log P_{o/w} = \log (C_o/C_w)$ , where  $C_o/C_w$  represents the concentration of complex in octanol/water phase.

### **Stability study**

The stabilities of **Ir1-Ir3** were investigated by UV-vis spectrophotometry. UV-vis absorption spectra of **Ir1-Ir3** and Chlorin e6 (all 20  $\mu\text{M}$ ) in Dulbecco's Modified Eagle Medium (DMEM) were recorded at room temperature and after keeping the solutions for 48 h in the dark or under light irradiation (465 nm, 6.5  $\text{mW}/\text{cm}^2$ ) for 30 min.

### **Singlet oxygen generation quantum yield measurements**

Singlet oxygen generation quantum yields ( $\Phi_{\Delta}$ ) of **Ir1-Ir3** were determined using a steady-state method with ABDA as the  $^1\text{O}_2$  probe and  $[\text{Ru}(\text{bpy})_3]\text{Cl}_2$  as the standard ( $\Phi_{\Delta} = 0.18$  in  $\text{H}_2\text{O}$ ). The solution, containing the tested complex and ABDA (300  $\mu\text{M}$ ) was prepared in the dark and then was irradiated with 465 nm light (power: 3.25  $\text{mW}/\text{cm}^2$ ) for 100 s. The absorbance of the solution was measured after each irradiation. The absorbance at 465 nm of the complex and  $[\text{Ru}(\text{bpy})_3]\text{Cl}_2$  was kept at 0.1. Mapping with the absorbance change of ABDA at 380 nm vs irradiation time, and singlet oxygen generation quantum yields ( $\Phi_{\Delta}$ ) of the complexes were calculated according to the following equation:

$$\Phi_{\Delta(x)} = \Phi_{\Delta(\text{std})} * (S_x/S_{\text{std}}) * (F_{\text{std}}/F_x)$$

where subscripts x and std designate the sample (complex) and  $[\text{Ru}(\text{bpy})_3]\text{Cl}_2$ , respectively; S stands for the slope of plot where time dependent absorbance of ABDA in 380 nm was plotted against the irradiation time (s). F stands for the absorption correction factor, which is given by  $F = 1 - 10^{-\text{OD}}$  (OD represents the optical density of sample and  $[\text{Ru}(\text{bpy})_3]\text{Cl}_2$  at irradiation wavelength).<sup>[3]</sup>

### **Photocatalytic reactions of compounds with NAD(P)H**

#### ***UV-Vis spectra***



Reactions between compounds and NAD(P)H at different ratios were monitored by UV-vis at room temperature in the dark or upon photo-irradiation with 465 nm (6.5 mW/cm<sup>2</sup>) light. Turnover number (TON) is defined as the number of moles of NAD(P)H that a mole of complex can convert within 30 min. Turnover frequency (TOF) was calculated from the difference in NAD(P)H concentration after 30 min irradiation divided by the concentration of complex. The concentration of NADH/NADPH was obtained using the extinction coefficient  $\epsilon_{339} = 6220 \text{ M}^{-1} \cdot \text{cm}^{-1}$  or  $\epsilon_{339} = 6300 \text{ M}^{-1} \cdot \text{cm}^{-1}$ . [4]

#### ***Detection of H<sub>2</sub>O<sub>2</sub> generation***

During the reaction of compounds with NAD(P)H in PBS solution at room temperature in the dark or after irradiation for 30 min, H<sub>2</sub>O<sub>2</sub> was detected by Quantofix<sup>®</sup> peroxide test sticks (Sigma).

#### **Cell culture**

HeLa and A549 cells were maintained in Dulbecco's Modified Eagle Medium (DMEM). B16 cells were grown in Roswell Park Memorial Institute medium (RPMI-1640). All media were supplemented with 10% v/v of fetal bovine serum (FBS), 1% v/v of 2 mM glutamine and 1% v/v penicillin/streptomycin. All the cells were incubated in a humidified incubator at 37 °C with 5% CO<sub>2</sub>.

#### **Cell viability assay**

Cytotoxicities of the tested compounds were determined by the MTT assay. Cells were seeded in 96-well flat-bottomed microplates (ca. 5000 cells/well) in growth medium (100  $\mu$ L) and incubated at 37 °C in a 5% CO<sub>2</sub> incubator for 24 h. Then fresh medium containing different concentrations of the compounds was added to each well for 48 h. Solutions of the complexes were initially prepared in DMSO and then were diluted with DMEM to make the final concentration of DMSO as 1%; for other *in vitro* cellular assays, the same procedure was followed. Wells containing untreated cells were used as blank controls. Then, MTT in PBS (10  $\mu$ L, 5 mg/mL) was added to each well and incubated for another 4 h at 37 °C. After that, the medium was removed and DMSO (100  $\mu$ L) was added to each well to dissolve the formed purple formazan. The absorbance of the solutions at 570 nm was measured with a Epoch<sup>™</sup> Microplate Spectrophotometer (BioTek). To test the phototoxicities of the compounds, cells were incubated with compounds for 16 h, followed by 5 min light irradiation with 465 nm (39 mW/cm<sup>2</sup>) light, and then incubation was continued for another 32 h. The IC<sub>50</sub> values for the compounds were determined from the dose-dependence cell-survival curve.

#### **Time dependent cellular uptake**

Cellular uptake of the complexes was investigated by determining the complex-based intracellular emission at different incubation times. HeLa cells (5 $\times$ 10<sup>4</sup> cells/mL) were cultured in twelve-well plates for 48 h. Then, the medium of the cells was changed to medium containing the complexes **Ir1-Ir3** (10  $\mu$ M) and incubated for 1 h, 2 h and 4 h respectively. Then the cells were washed twice

with PBS and harvested. The intracellular emission intensity of the complexes was measured by flow cytometry (CytoFLEX of Beckman Coulter).

### **Cellular localization assay**

HeLa cells were seeded in 35 mm glass bottom dishes (Corning) and allowed to adhere for 48 h. The cells were then incubated with **Ir1-Ir3** (10  $\mu$ M) at 37 °C for 2 h and then further co-incubated with the commercial lysosomal probe Lyso Tracker<sup>®</sup>Deep Red (LTDR, 100 nM) or mitochondrial probe Mito Tracker<sup>®</sup>Red (MTR, 100 nM) for additional 30 min. The cells were washed with PBS once and visualized by using a LSM 880 laser confocal microscope (Carl Zeiss, Germany) immediately. The excitation wavelengths for **Ir1**, **Ir2**, **Ir3**, LTDR and MTR are 405, 458, 488, 633 and 633 nm, respectively. Emission filter: 500  $\pm$  40 nm (for **Ir1**), 540  $\pm$  40 nm (for **Ir2**), 580  $\pm$  40 nm (for **Ir3**), 680  $\pm$  20 nm (for LTDR), and 680  $\pm$  20 nm (for MTR).

### **Intracellular <sup>1</sup>O<sub>2</sub> detection**

HeLa cells were seeded at a density of 5000 cells/well of a 96-well plate for 48 h. Then, the cells were incubated with different concentrations of **Ir1-Ir3** for 2 h, followed by irradiation with light (465 nm, 39 mW/cm<sup>2</sup>) for 5 min. After that, cells were stained with 5  $\mu$ M of singlet oxygen sensor green (SOSG, <sup>1</sup>O<sub>2</sub> specific probe) for 30 min and then the fluorescence images were immediately captured using a fluorescence microscope.

### **Intracellular O<sub>2</sub><sup>•-</sup> detection**

HeLa cells were seeded at a density of 5000 cells/well of a 96-well plate for 48 h. Then, the cells were incubated with different concentrations of **Ir1-Ir3** for 2 h, followed by light irradiation (465 nm, 39 mW/cm<sup>2</sup>) for 5 min. After that, dihydroethidium (DHE, O<sub>2</sub><sup>•-</sup> specific probe, 5  $\mu$ M) was added and then incubated for 30 min at 37 °C. The fluorescence images were immediately acquired with a fluorescence microscope.

### **Detection of mitochondrial membrane potential**

Change in the mitochondrial membrane potential was monitored by JC-1 assay. Briefly, HeLa cells were seeded at a density of 5000 cells/well of a 96-well plate for 48 h. The cells were incubated with various concentrations of **Ir1-Ir3** for 2 h, and then irradiated with light (465 nm, 39 mW/cm<sup>2</sup>) for 5 min. After another 1 h incubation in the dark at 37 °C, the JC-1 was added and then incubated for 20 min at 37 °C. Then cells were washed once with PBS, followed by the imaging by a fluorescence microscope.

### **Annexin V-FITC/PI assay by fluorescence microscopy**

HeLa cells were incubated with different concentrations of **Ir1-Ir3** for 4 h and then irradiated with 465 nm LED (39 mW/cm<sup>2</sup>) for 5 min. After removing the medium, the cells were stained with

annexin V-FITC (2.5  $\mu$ L) and PI (2.5  $\mu$ L) in the binding solution for 15 min. Then, the fluorescence images were obtained using a fluorescence microscope.

#### **Annexin V-FITC/PI assay using flow cytometry**

HeLa cells were incubated with **Ir3** for 4 h and then irradiated with 465 nm LED (39 mW/cm<sup>2</sup>) for 5 min. After removing the medium, the cells were collected by centrifugation, and stained with annexin V-FITC (5  $\mu$ L) and PI (10  $\mu$ L) in the binding solution for 15 min. Then, the apoptosis and necrosis of HeLa cells were monitored by flow cytometry.

#### **Photo-cytotoxicity against 3D MCTSs<sup>[5]</sup>**

##### ***Multicellular tumor spheroids (MCTSs) formation***

Approximately, 500 HeLa cells were transferred to 0.75% agarose-coated transparent 96-well plates with 200  $\mu$ L of culture media. The cells were then re-suspended in culture media and incubated. MCTSs aggregates of ca. 400  $\mu$ m were formed after 8 days. Half of the culture medium was carefully refreshed in every four days.

##### ***Z-stack scanning of MCTSs***

MCTSs (diameter: ca. 400  $\mu$ m) were incubated with 5  $\mu$ M of **Ir3** for 24 h in the dark, washed carefully with PBS, and transferred to 35 mm glass bottom dishes (Corning) and then were subjected to CLSM for the Z-stack imaging study. The luminescence images of each section along the Z-axis were captured with an interval of 22  $\mu$ m in “Z-stack scanning” mode. The excitation wavelength was set at 488 nm, and the emission signals were collected in the range of 580  $\pm$  40 nm.

##### ***Growth inhibition assay of MCTSs***

MCTSs (diameter: ca. 400  $\mu$ m) were divided into three groups and treated with either of the culture medium or 50  $\mu$ M cisplatin or 5  $\mu$ M **Ir3**. MCTSs were treated by carefully replacing 50% of the medium with drug-supplemented medium. In parallel, 50% of the solvent-containing medium was replaced by solvent-free medium for the untreated MCTSs. After this, the MCTSs were divided into dark and light groups. After incubating in the dark for 24 h, the MCTSs of light group were exposed to a 465 nm LED lamp (39 mW/cm<sup>2</sup>) for 5 min. The cell culture media was replaced every four days. The integrity and diameter of the MCTSs were monitored with an inverted fluorescence microscope every four days, and the MCTSs volumes were evaluated with the spherical volume formula:  $V = 4/3\pi r^3$ .

#### ***In-vivo biological studies***

##### ***Zebrafish studies***

Zebrafish experiments were carried out under the Laboratory Animal Center, Sun Yet-Sen University, Guangzhou, China, using the wild-type zebrafish (AB) embryos (< 10 hpf) and *Tg(flk1:EGFP)<sup>s843</sup>* zebrafish embryos <sup>[6]</sup>(< 10 hpf). All animals were maintained in accordance with ASPA 1986 and conducted in accordance with the guidelines and approval of the respective Animal

Research and Ethics Committees of the Sun Yat-Sen University. Zebrafish were housed in  $28 \pm 0.5$  °C, and were monitored at least once in a day. Regular system checks were carried out daily to ensure water quality and parameters are maintained. Light cycle: 14 hours day, 10 hours night.<sup>[7]</sup>

#### ***Development and survival of zebrafish embryos and larvae***

24-well plates were prepared with 3 concentrations of **Ir3** (typically 0.01, 0.1 and 1  $\mu$ M, 1 ml per well) in triplicate. DMSO was used to solubilize the complexes and did not exceed 0.1% v/v in the final solutions. The plates were seeded with 6 embryos (AB-type) per well, then incubated for 96 h at  $28 \pm 0.5$  °C. Untreated embryos were also incubated for 96 h (as the negative control samples). Development and survival of embryos were recorded every 24 h using a microscope. Larvae (AB-type) were treated in the same method as embryos.

#### ***Observation on morphological abnormalities and blood vessels of zebrafish larvae***

To determine the effects of **Ir3** on the spinal column curving and blood vessels of larvae, 2-days-old *Tg(flk1:EGFP)<sup>s843</sup>* zebrafish larvae were exposed to 0.1 and 1  $\mu$ M **Ir3** for 96 h at  $28 \pm 0.5$  °C. Triplicate were set and six larvae were used for each replicate. The spinal column curving of larvae was recorded every 24 h using a fluorescence microscope.

## **Tables**

**Table S1.** Solubility of **Ir1-Ir4** in H<sub>2</sub>O at 25 °C.

	<b>Compound</b>			
	<b>Ir1</b>	<b>Ir2</b>	<b>Ir3</b>	<b>Ir4</b>
<b>S (mg/ml H<sub>2</sub>O, 25 °C)</b>	$130 \pm 6$	$110 \pm 5$	$3 \pm 0.2$	$0.5 \pm 0.2$
<b>(mM)</b>	(155)	(114)	(2.5)	(0.5)

**Table S2.** Emission quantum yields ( $\Phi$ ) of **Ir1-Ir3** in H<sub>2</sub>O and CH<sub>3</sub>CN. [Ru(bpy)<sub>3</sub>]Cl<sub>2</sub> was used as standard. (Excitation: 465 nm)

<b>Complex</b>	<b>Solvent</b>	<b><math>\Phi</math> (aerated)</b>	<b><math>\Phi</math> (deaerated)</b>
<b>Ir1</b>	H <sub>2</sub> O	0.037	0.087
	CH <sub>3</sub> CN	0.011	0.453
<b>Ir2</b>	H <sub>2</sub> O	0.060	0.067
	CH <sub>3</sub> CN	0.019	0.138
<b>Ir3</b>	H <sub>2</sub> O	0.004	0.046
	CH <sub>3</sub> CN	0.004	0.154

**Table S3.** Octanol-water partition coefficient log P<sub>o/w</sub> of **Ir1-Ir3**.

<b>Compound</b>	<b>Ir1</b>	<b>Ir2</b>	<b>Ir3</b>	<b>Ir4</b>
-----------------	------------	------------	------------	------------

<b>Log P<sub>o/w</sub></b>	0.18 ± 0.01	0.31 ± 0.02	0.32 ± 0.03	1.34 ± 0.08
----------------------------	-------------	-------------	-------------	-------------

**Table S4.** Singlet oxygen generation quantum yield ( $\Phi_{\Delta}$ ) of **Ir1-Ir3** in aqueous solution. [Ru(bpy)<sub>3</sub>]Cl<sub>2</sub> was used as the standard.

<b>Compound</b>	<b>Ir1</b>	<b>Ir2</b>	<b>Ir3</b>
$\Phi_{\Delta}$	0.06	0.39	0.23

**Table S5.** Turnover numbers (TONs) and turnover frequencies (TOFs) of compounds for NADH (160  $\mu$ M)/NADPH (160  $\mu$ M) photo-oxidation after 30 min irradiation with 465 nm blue light.

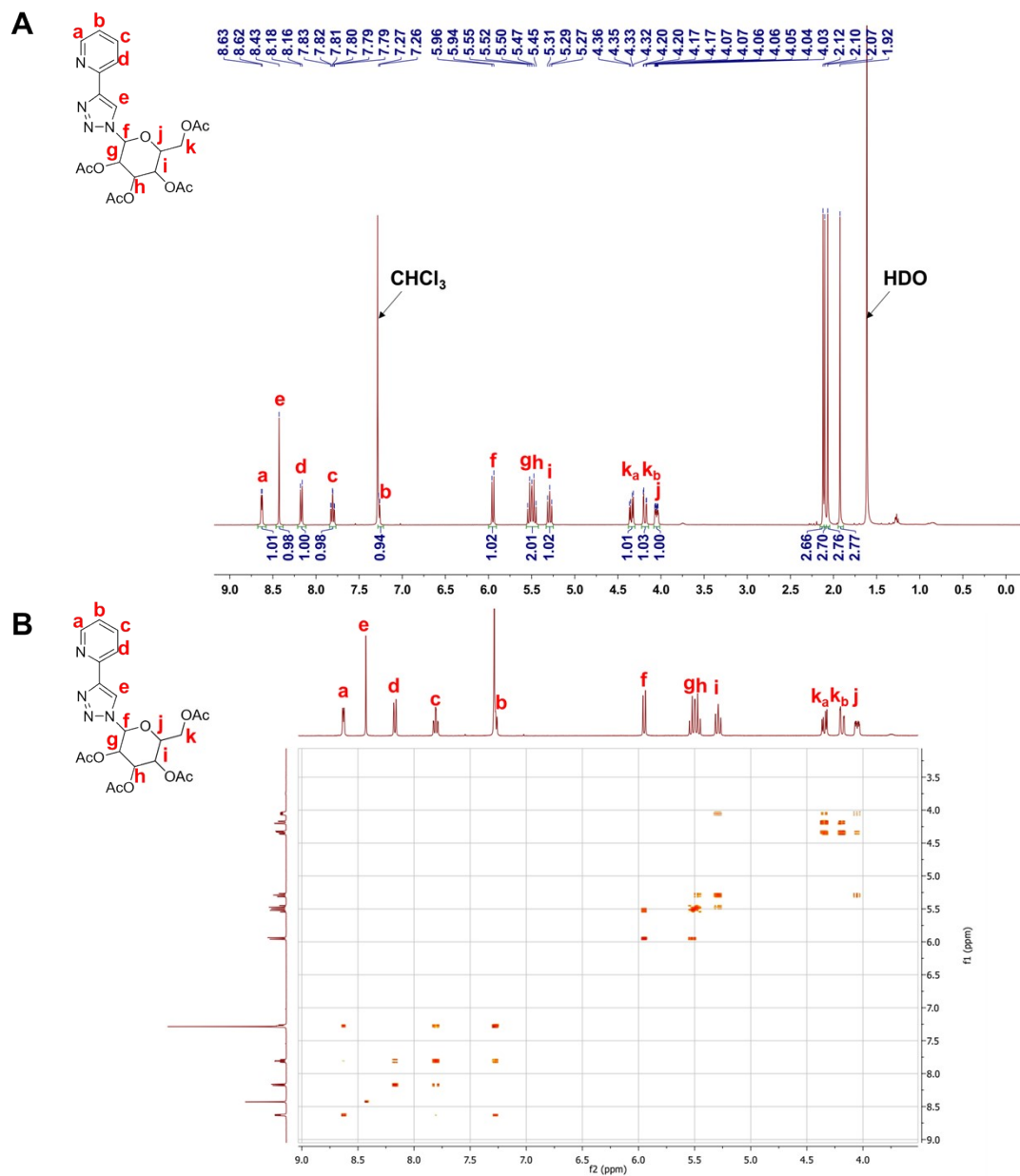
<b>Compound</b>	<b>Concentration (<math>\mu</math>M)</b>	<b>Coenzymes</b>	<b>TON</b>	<b>TOF (h<sup>-1</sup>)</b>
<b>Ir1</b>	5	NADH	8.4	16.9
		NADPH	6.9	13.8
<b>Ir2</b>	5	NADH	21.4	42.8
		NADPH	19.0	38.1
<b>Ir3</b>	0.5	NADH	207.1	414.2
		NADPH	203.3	406.6
<b>Ce6</b>	5	NADH	24.5	49.0
		NADPH	23.9	47.8

**Table S6.** IC<sub>50</sub> values ( $\mu$ M) and photo-cytotoxicity indices (PI) of compounds against A549 lung and B16 melanoma cancer cells monolayer.

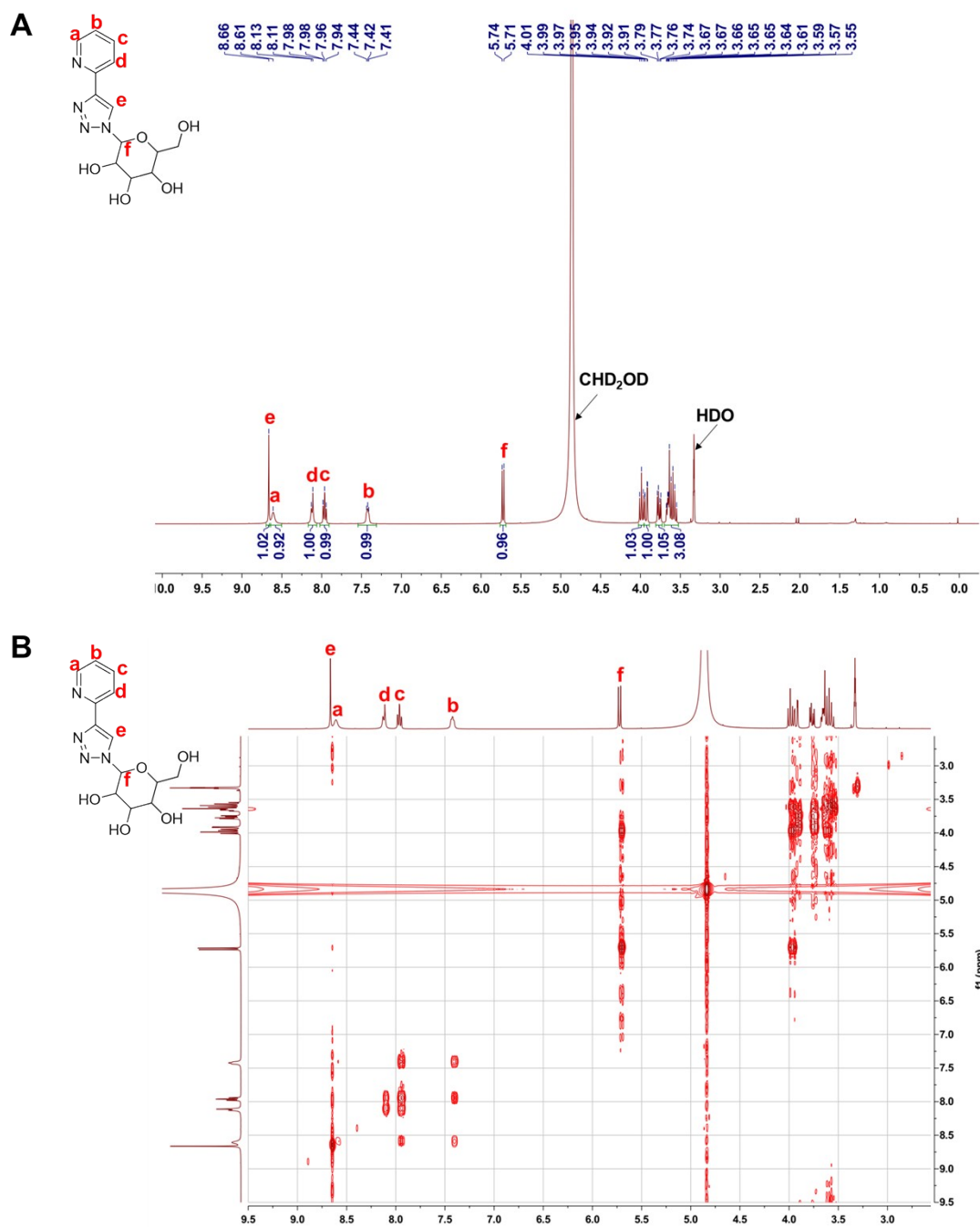
<b>Cell lines</b>	<b>Compound</b>	<b>IC<sub>50</sub> (<math>\mu</math>M)</b>		
		<b>Dark<sup>a</sup></b>	<b>Light<sup>b</sup></b>	<b>PI</b>
<b>A549</b>	<b>Ir1</b>	>100	18.6 ± 0.2	>5.4
	<b>Ir2</b>	37.5 ± 1.2	0.9 ± 0.03	41.7
	<b>Ir3</b>	55.0 ± 1.3	0.2 ± 0.01	275.0
	<b>5-ALA</b>	>1000	151.2 ± 3.4	>6.6
	<b>Cisplatin</b>	10.5 ± 0.8	9.9 ± 0.2	1.1
<b>B16</b>	<b>Ir1</b>	>100	1.8 ± 0.09	>55.6
	<b>Ir2</b>	4.5 ± 0.2	0.05 ± 0.002	90.0
	<b>Ir3</b>	0.8 ± 0.03	0.002 ± 0.0001	400.0
	<b>5-ALA</b>	>1000	118.3 ± 2.5	>8.5
	<b>Cisplatin</b>	31.0 ± 2.5	44.7 ± 3.4	n.a <sup>c</sup>

<sup>a</sup>48 h drug exposure followed by incubation at 37 °C, 5% CO<sub>2</sub> in the dark. <sup>b</sup>16 h drug exposure, followed by light irradiation (465 nm, 39 mW/cm<sup>2</sup>) 5 min and then 32 h incubation at 37 °C, 5%

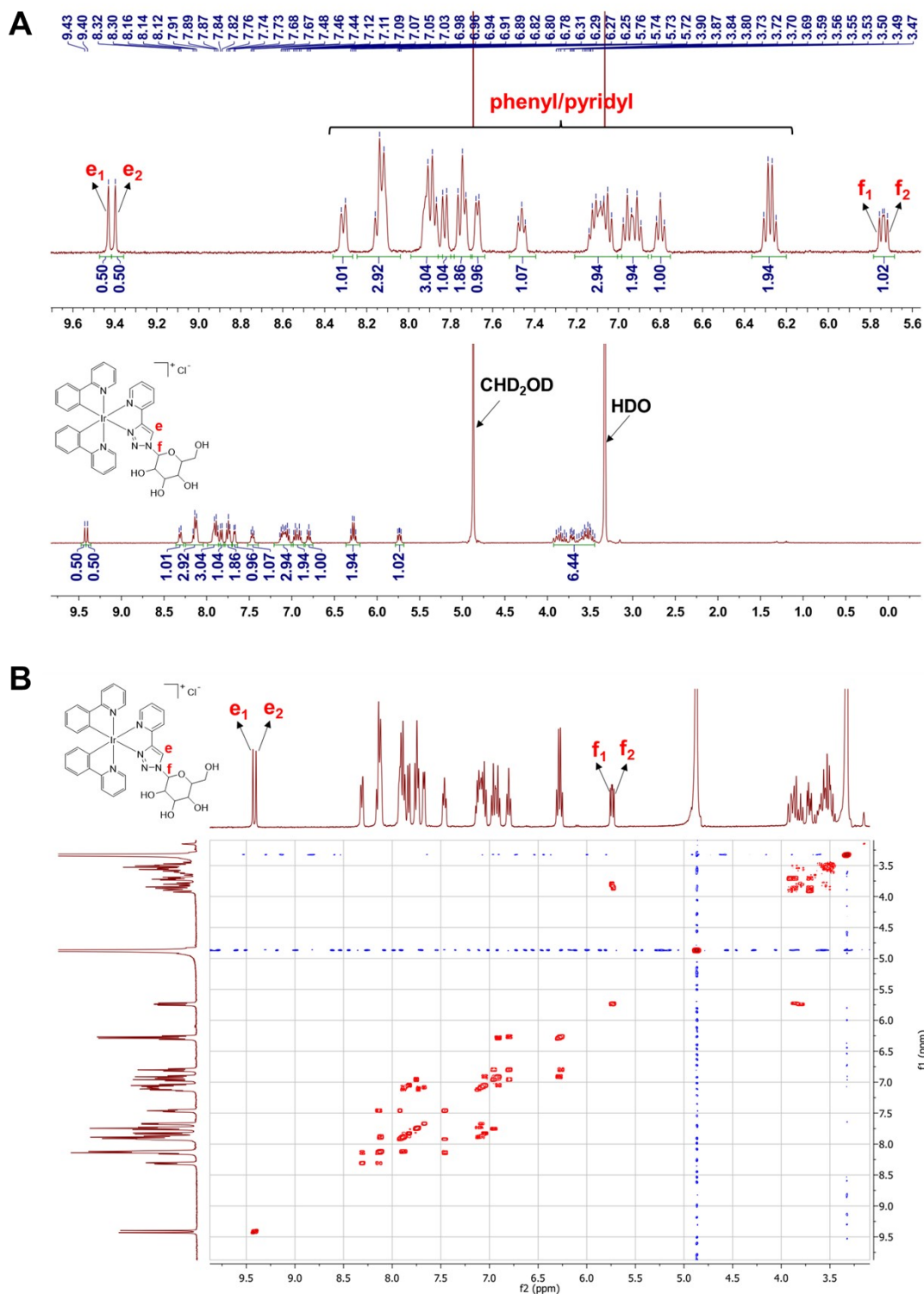
## Figures



**Fig. S1.** <sup>1</sup>H NMR spectrum (400 MHz, chloroform-*d*) (A) and <sup>1</sup>H-<sup>1</sup>H 2D COSY spectrum (400 MHz, chloroform-*d*) (B) of GlcOAc ligand.

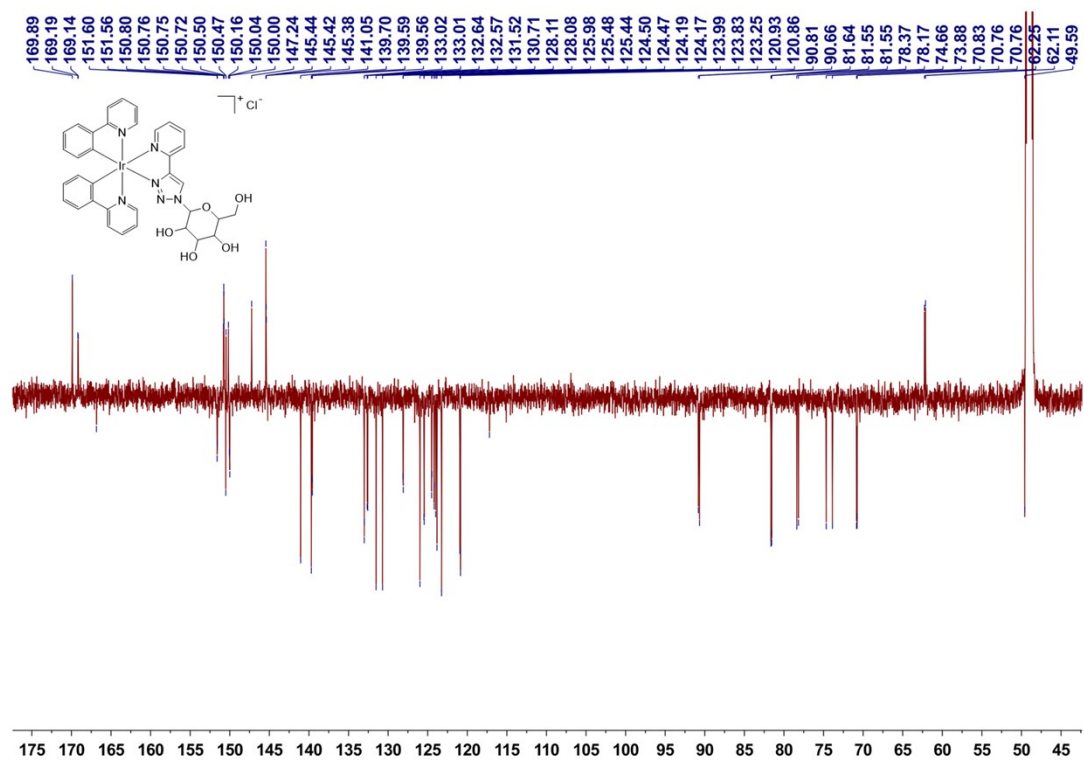


**Fig. S2.**  $^1\text{H}$  NMR spectrum (400 MHz, methanol- $d_4$ ) (A) and  $^1\text{H}$ - $^1\text{H}$  2D COSY spectrum (400 MHz, methanol- $d_4$ ) (B) of GlcOH ligand.

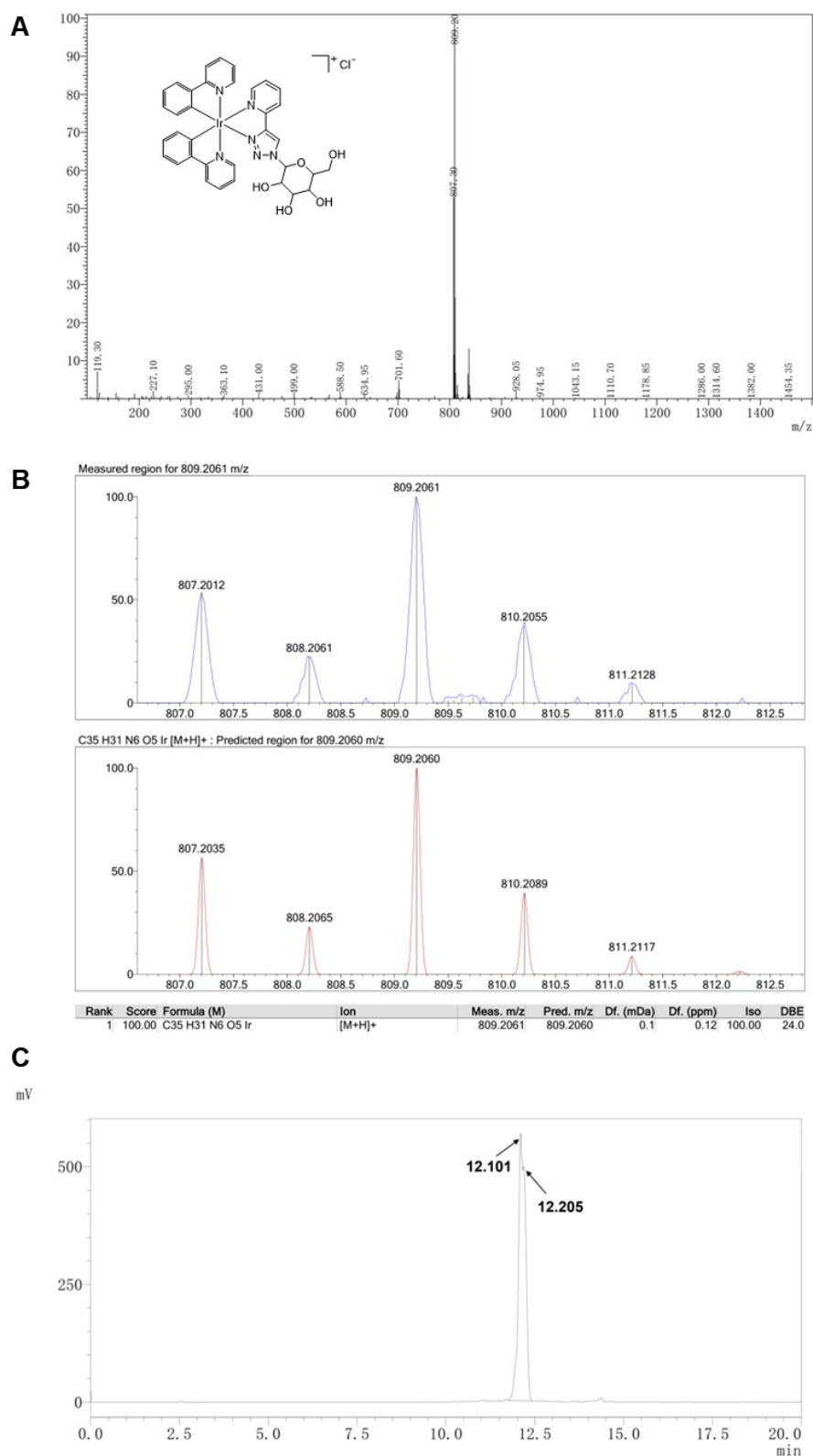


**Fig. S3.**  $^1\text{H}$  NMR (400 MHz, methanol- $d_4$ ) spectrum (A) and  $^1\text{H}$ - $^1\text{H}$  2D COSY spectrum (400 MHz, methanol- $d_4$ ) (B) of **Ir1**. Proton e consists of two singlets (no coupling in COSY), and are assignable to the presence of two diastereomers, which complicates the unambiguous assignment of other peaks.

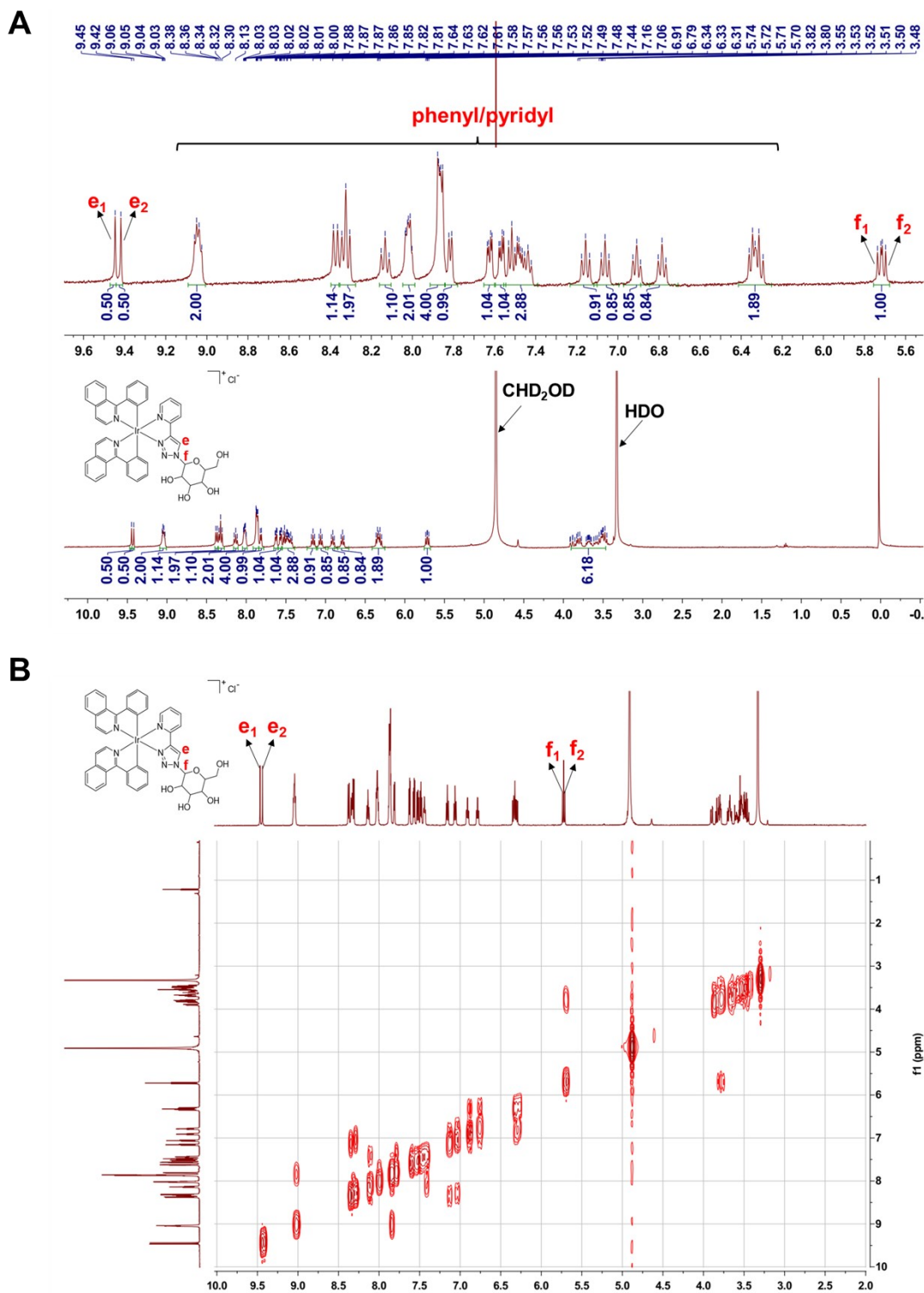


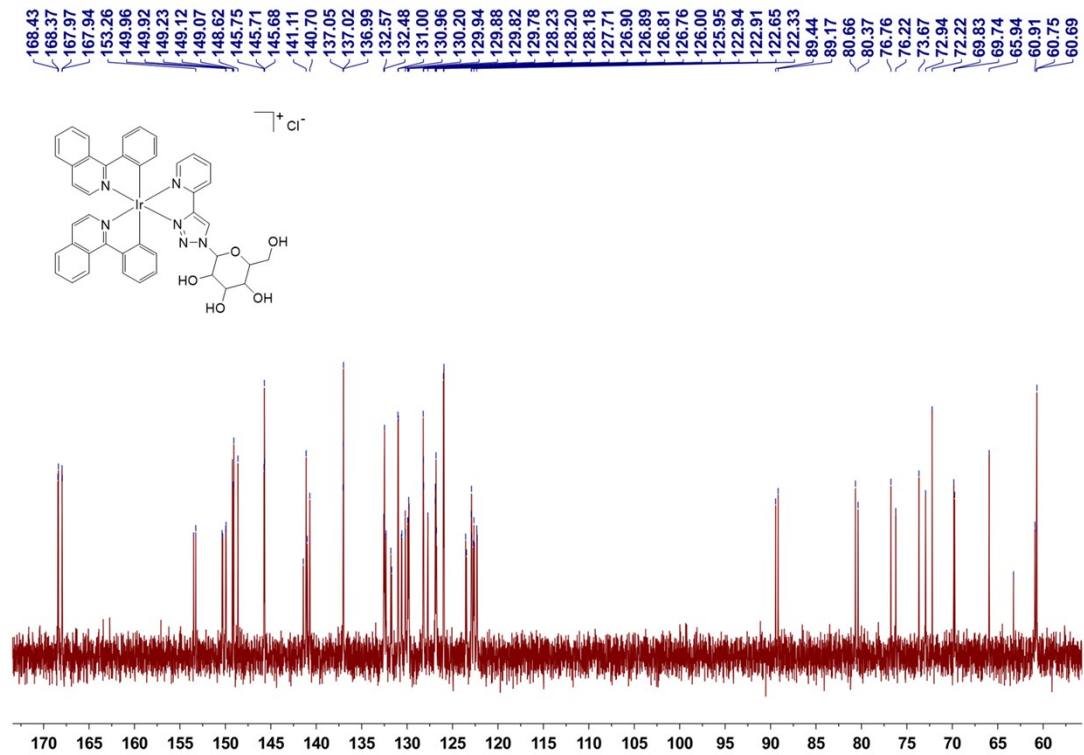


**Fig. S4.**  $^{13}\text{C}$  APT NMR spectrum (150 MHz, methanol- $d_4$ ) of **Ir1**. The presence of diastereomers is evident from the doubling of some peaks (many of which are overlapped).

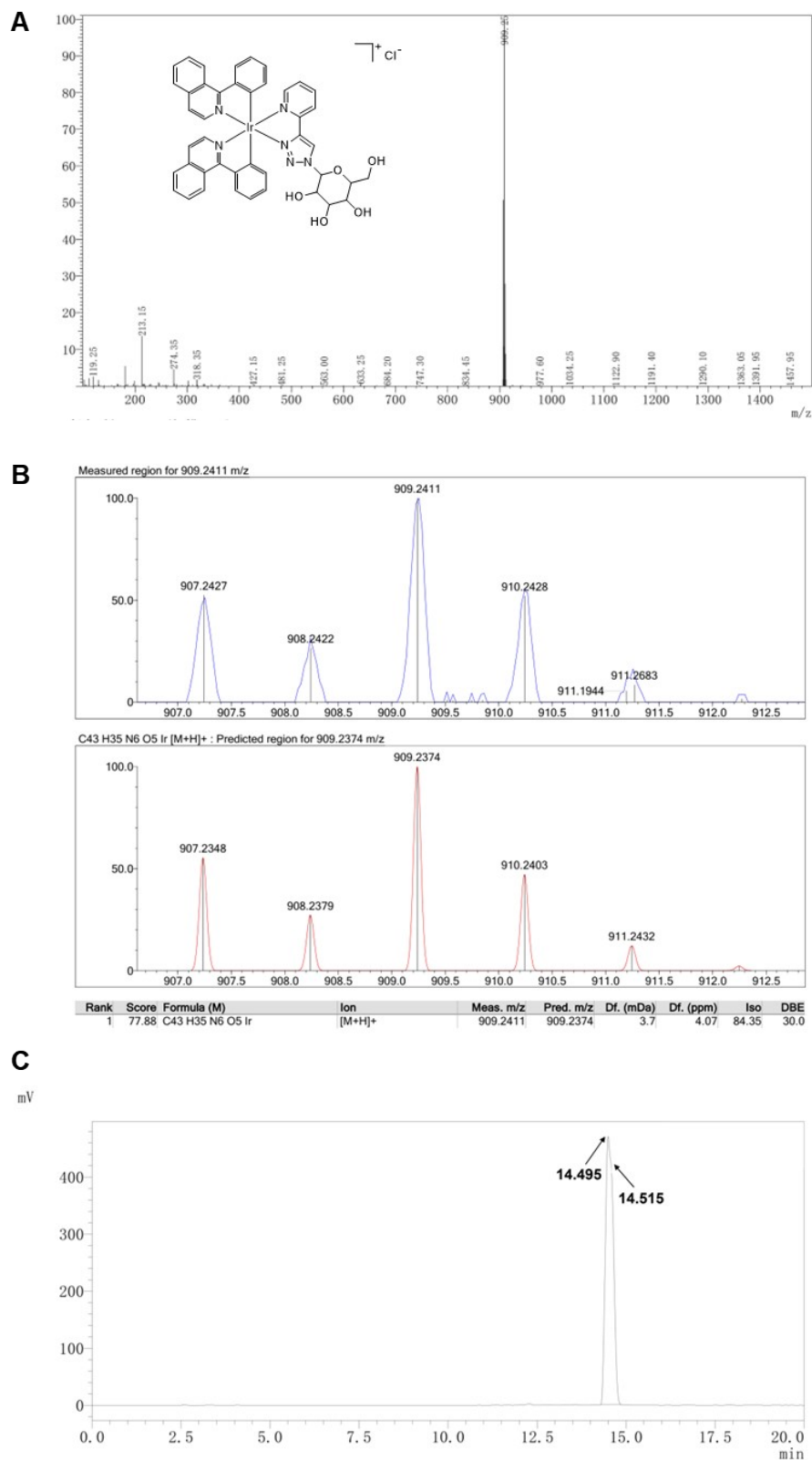


**Fig. S5.** ESI-MS (A), HRMS spectrum (B) and HPLC trace (99.5% purity by peak area) (C) of **Ir1**. **Ir1** shows only one mass peak while the reverse phase HPLC reflects the slightly different retention times of the two diastereomers.

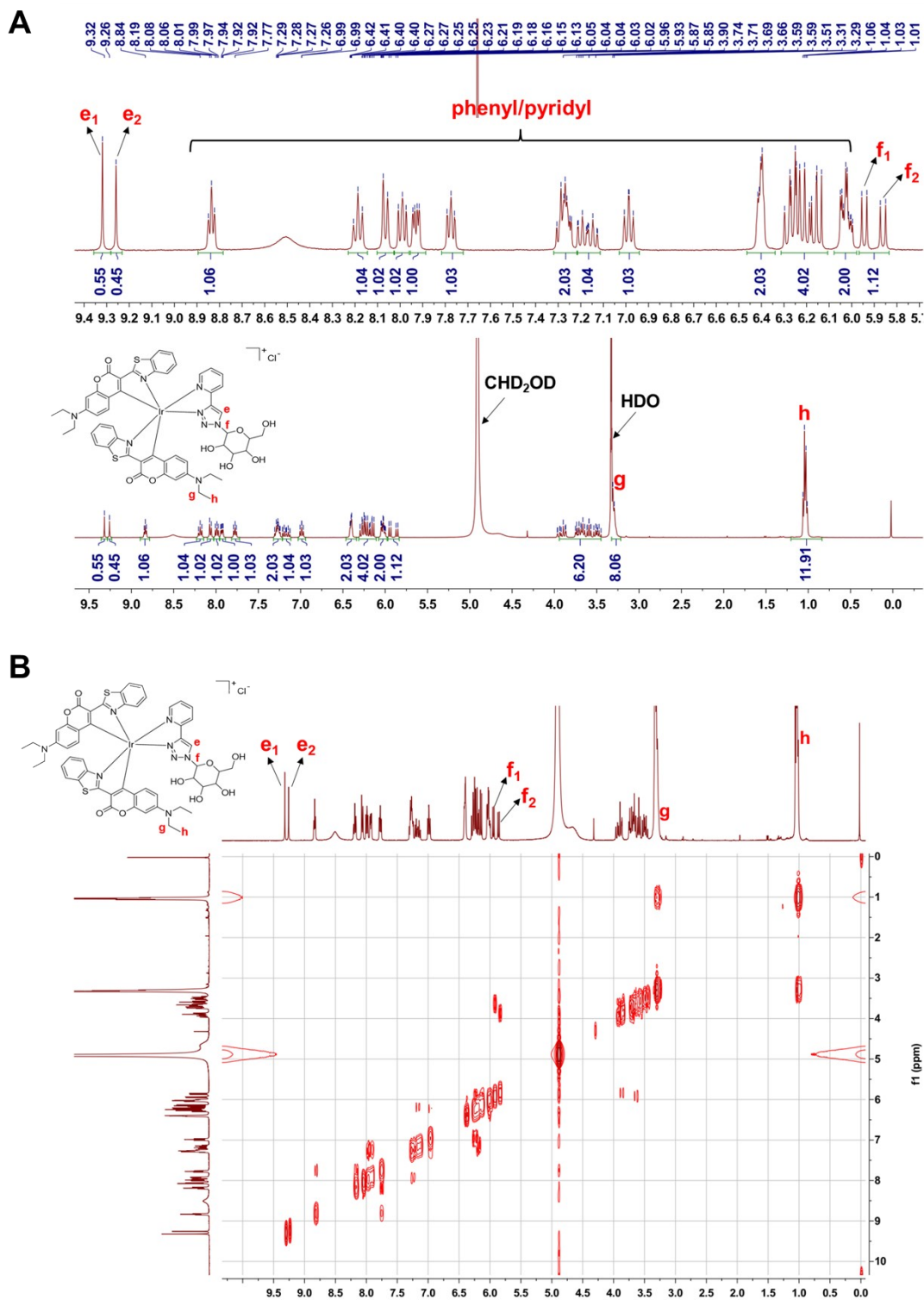




**Fig. S7.**  $^{13}\text{C}$  NMR spectrum (100 MHz,  $\text{DMSO-}d_6$ ) of **Ir2**. The presence of diastereomers is evident from the doubling of some peaks (many of which are overlapped).



**Fig. S8.** ESI-MS (A), HRMS spectrum (B) and HPLC trace (99.8% purity by peak area) (C) of **Ir2**. **Ir2** shows only one mass peak while the reverse phase HPLC reflects the slightly different retention times of the two diastereomers.



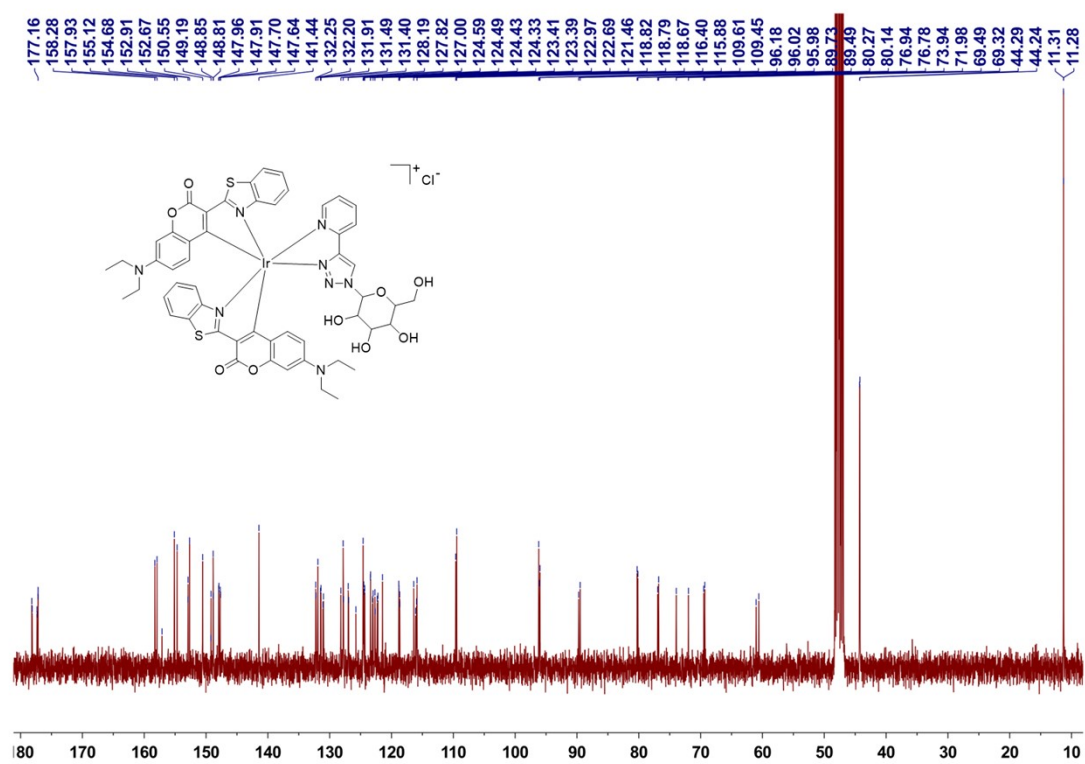


**Fig. S10.**  $^{13}\text{C}$  NMR spectrum (100 MHz,  $\text{methanol-}d_4$ ) of **Ir3**. The presence of diastereomers is evident from the doubling of some peaks (many of which are overlapped).

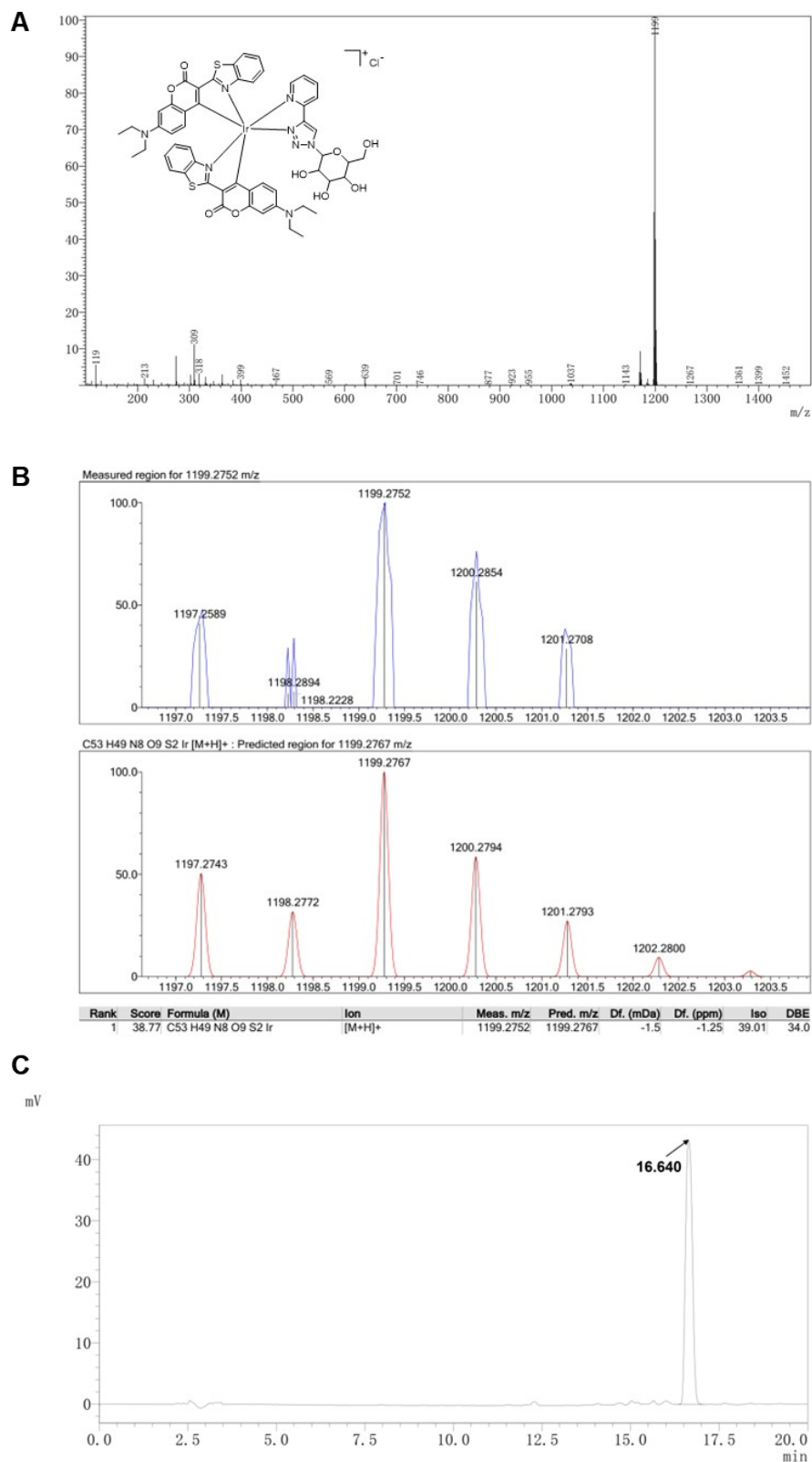


**Fig. S11.** ESI-MS (A), HRMS spectrum (B) and HPLC trace (96.2% purity by peak area) (C) of **Ir3**. **Ir3** shows only one mass peak and the reverse phase HPLC does not separate the two diastereomers.



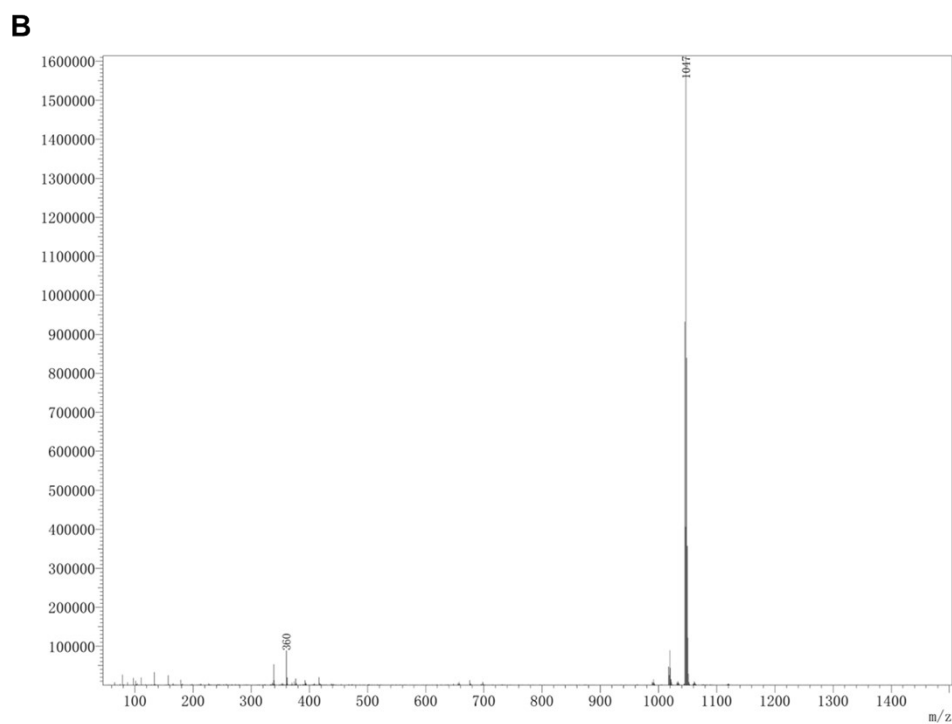
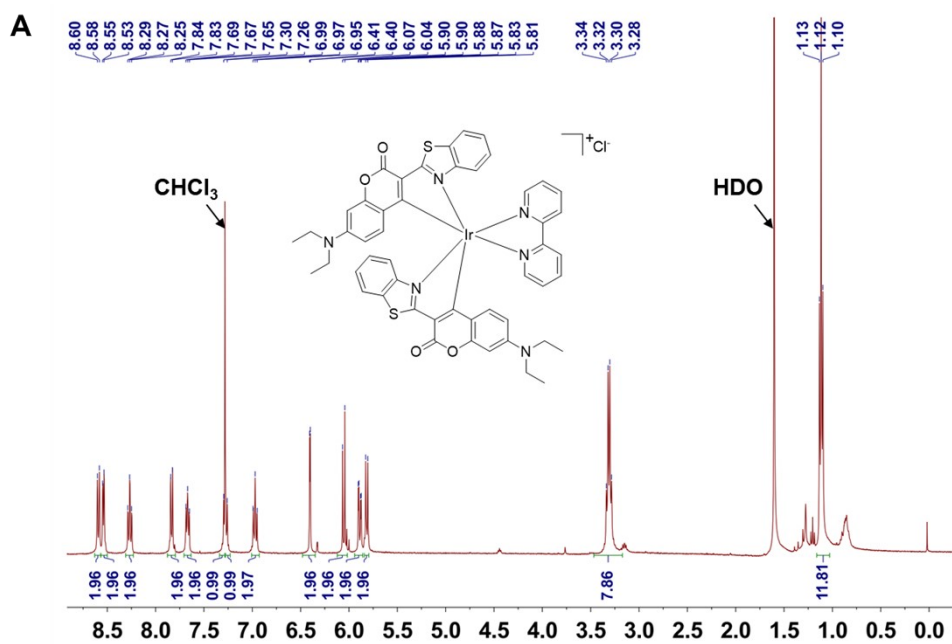


**Fig. S12.**  $^1\text{H}$  NMR (400 MHz, chloroform- $d$ ) spectrum (A) and ESI-MS spectrum (B) of Ir4.

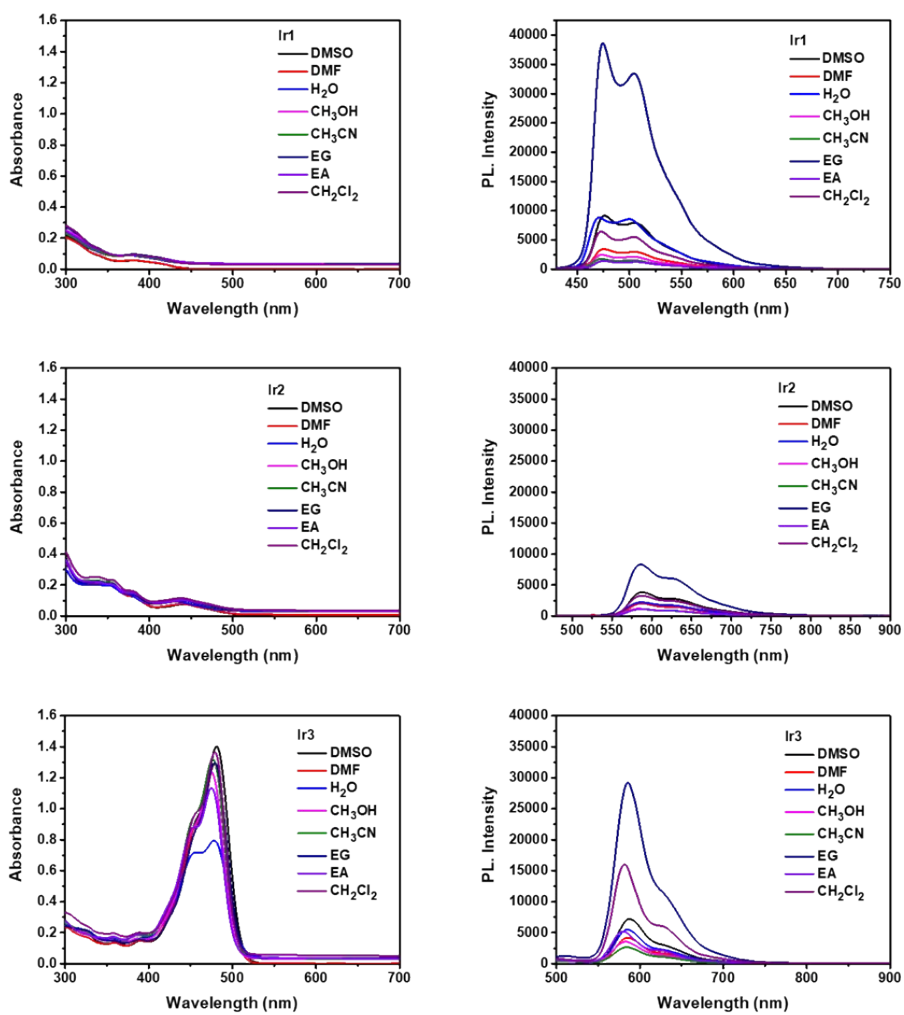


**Fig. S13.** UV-visible absorption (left) and emission (right) spectra of **Ir1** ( $\lambda_{\text{ex}} = 405 \text{ nm}$ ), **Ir2** ( $\lambda_{\text{ex}} = 458 \text{ nm}$ ) and **Ir3** ( $\lambda_{\text{ex}} = 488 \text{ nm}$ ) ( $10 \mu\text{M}$ ) in various solvents at room temperature.

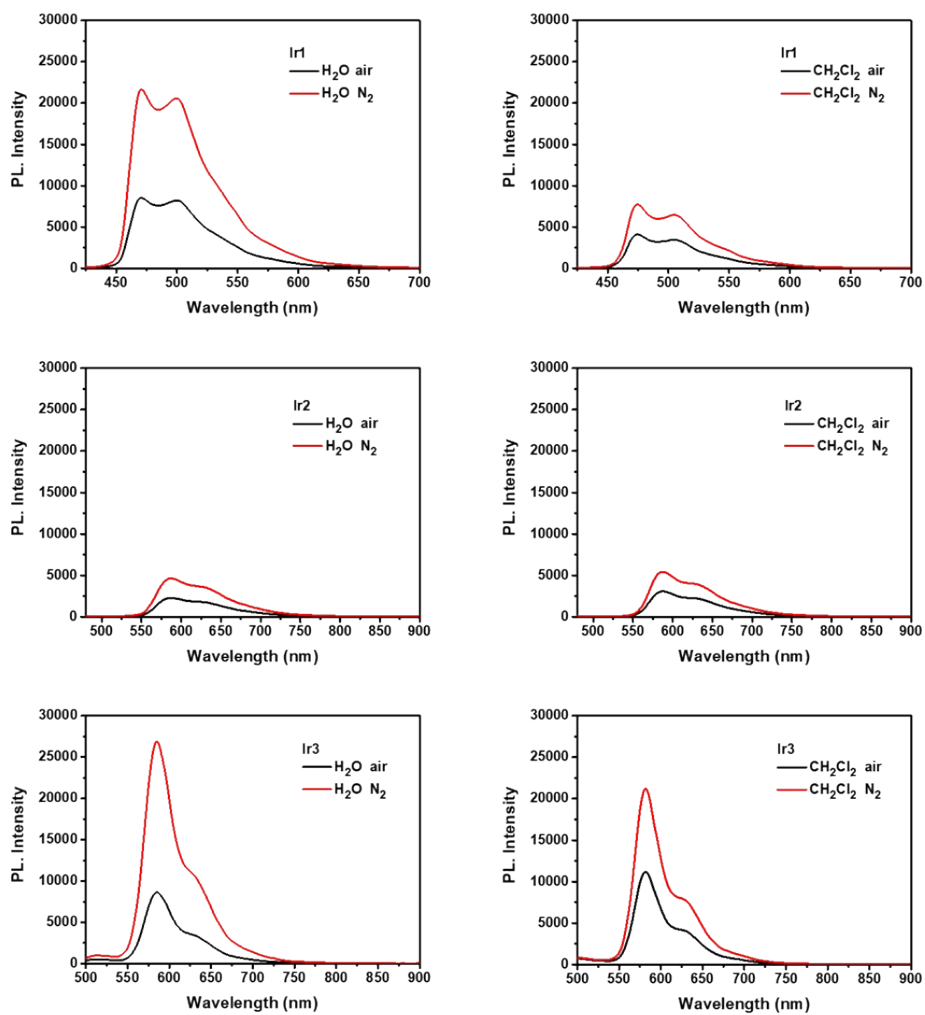


**Fig. S14.** Phosphorescence spectra of **Ir1** ( $\lambda_{\text{ex}} = 405$  nm), **Ir2** ( $\lambda_{\text{ex}} = 458$  nm) and **Ir3** ( $\lambda_{\text{ex}} = 488$  nm) (10  $\mu\text{M}$ ) in air or nitrogen-saturated H<sub>2</sub>O and CH<sub>2</sub>Cl<sub>2</sub> at room temperature.

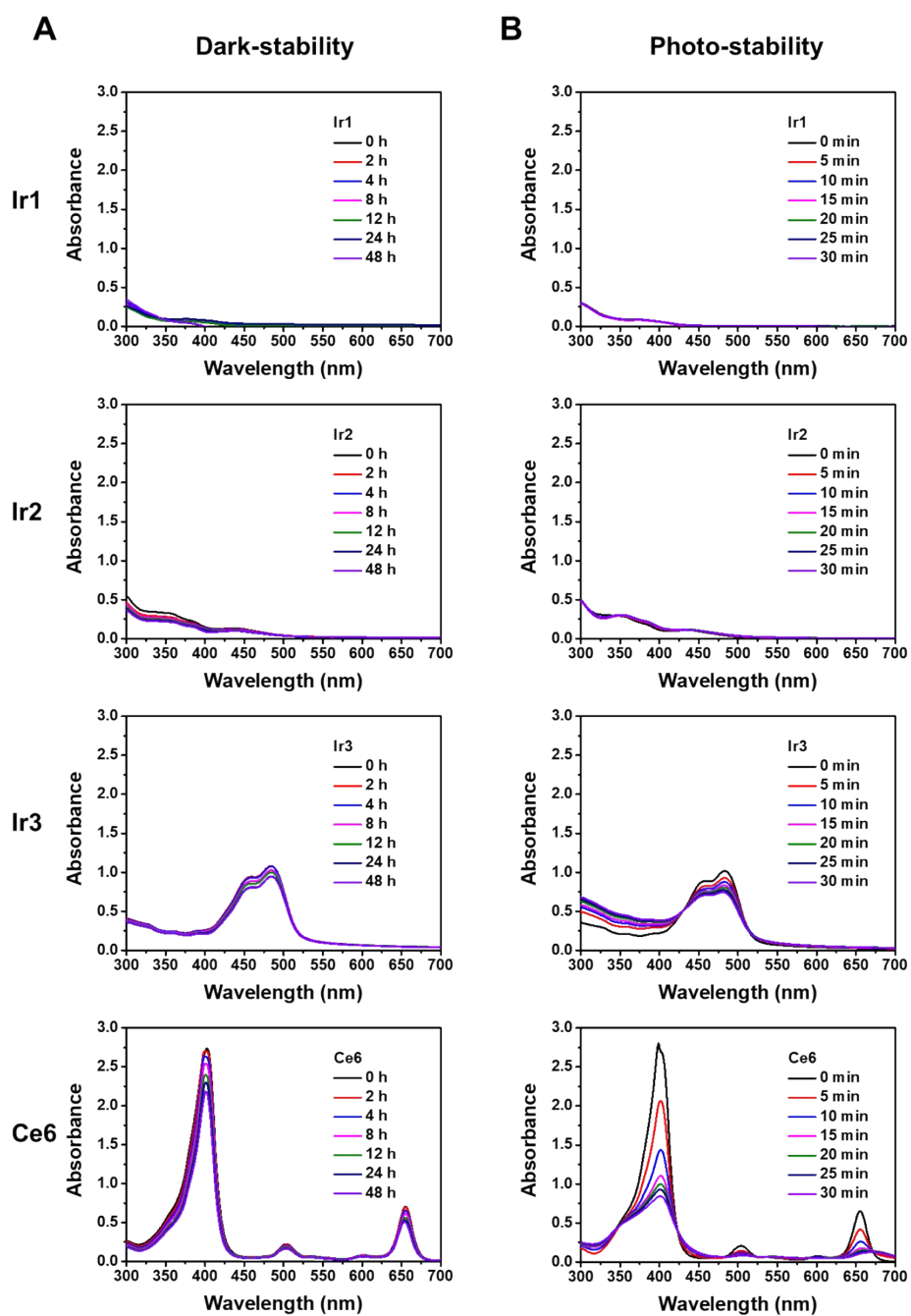


**Fig. S15.** UV-vis absorption spectra of **Ir1-Ir3** and Chlorin e6 (20  $\mu$ M) after 48 h in the dark, or blue light irradiation (465 nm, 6.5 mW/cm<sup>2</sup>) for 30 min to indicate the dark- and photo-stability in Dulbecco's Modified Eagle Medium (DMEM).

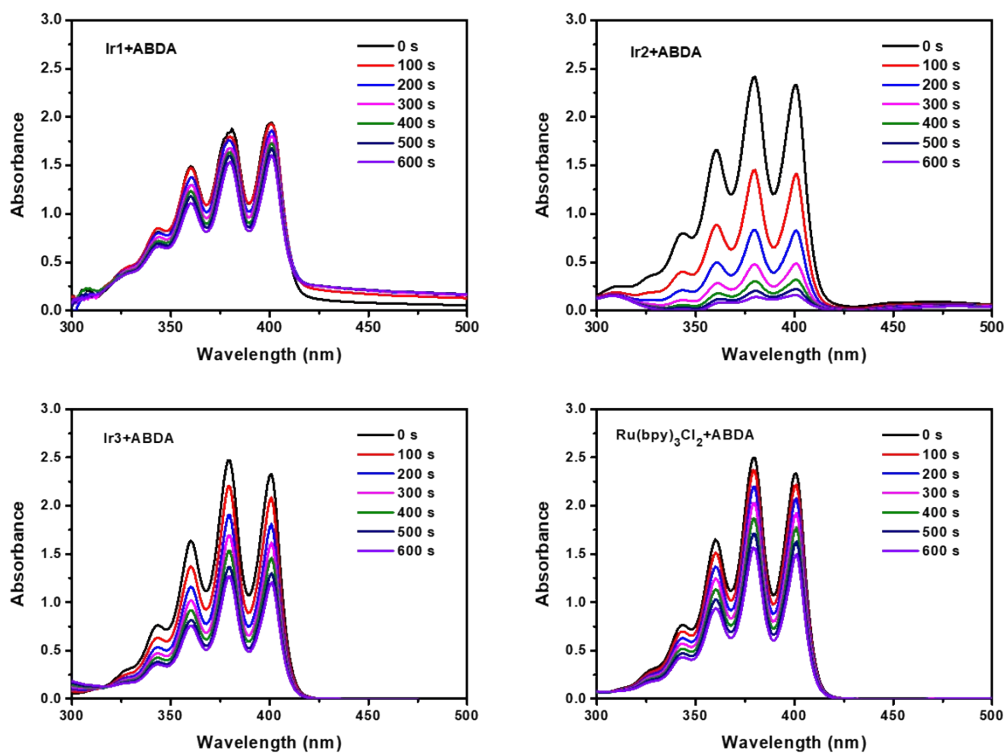


**Fig. S16.** Determination of <sup>1</sup>O<sub>2</sub> production of **Ir1-Ir3** by monitoring the time-dependent UV-vis absorption spectra of ABDA after treatment with **Ir1-Ir3** or [Ru(bpy)<sub>3</sub>]Cl<sub>2</sub> standard. Conditions: 465 nm LED lamp (irradiance: 3.25 mW/cm<sup>2</sup>).

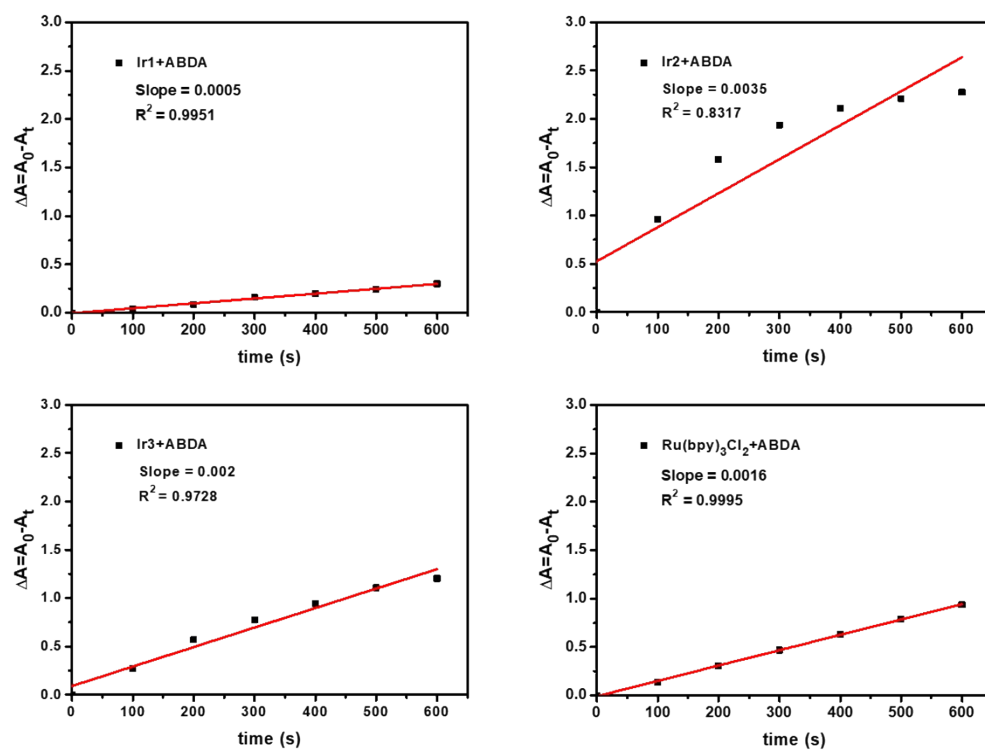


**Fig. S17.** Plot of the change in absorbance of ABDA at 380 nm against the irradiation time (s). Conditions: 465 nm LED lamp (irradiance: 3.25 mW/cm<sup>2</sup>).

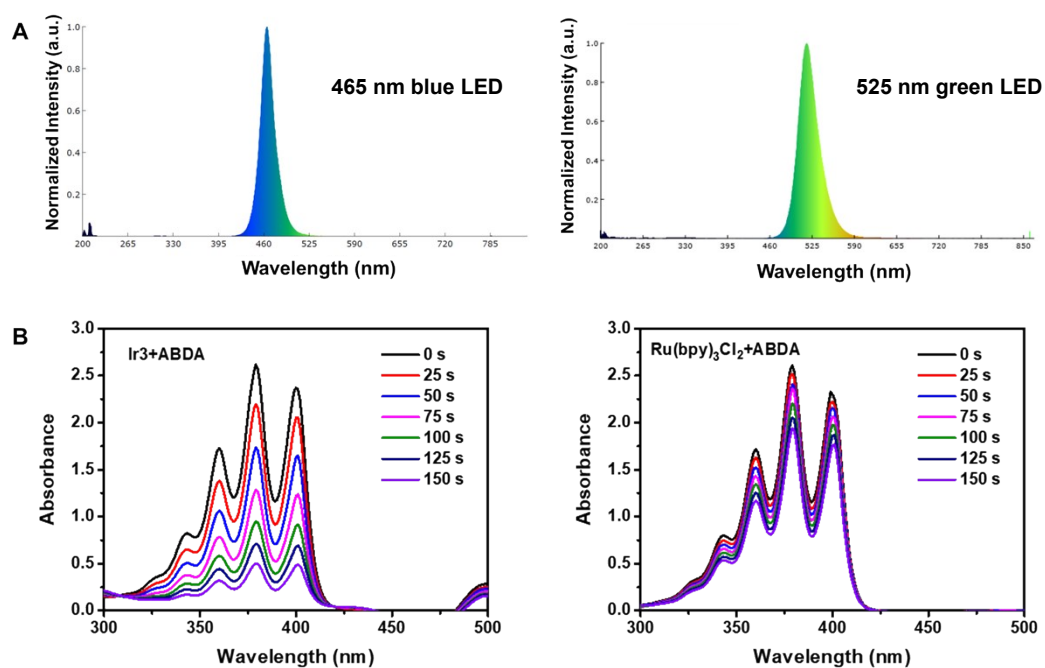


**Fig. S18.** (A) The emission spectra of the 465 nm blue LED and 525 nm green LED. The broad spectrum of the 525 nm LED overlaps with the UV-vis spectrum of **Ir3**. (B) Determination of <sup>1</sup>O<sub>2</sub> production by **Ir3** under 525 nm green light irradiation (irradiance: 4.8 mW/cm<sup>2</sup>) by monitoring the time-dependent UV-vis absorption spectrum of ABDA. [Ru(bpy)<sub>3</sub>]Cl<sub>2</sub> was used as a standard.

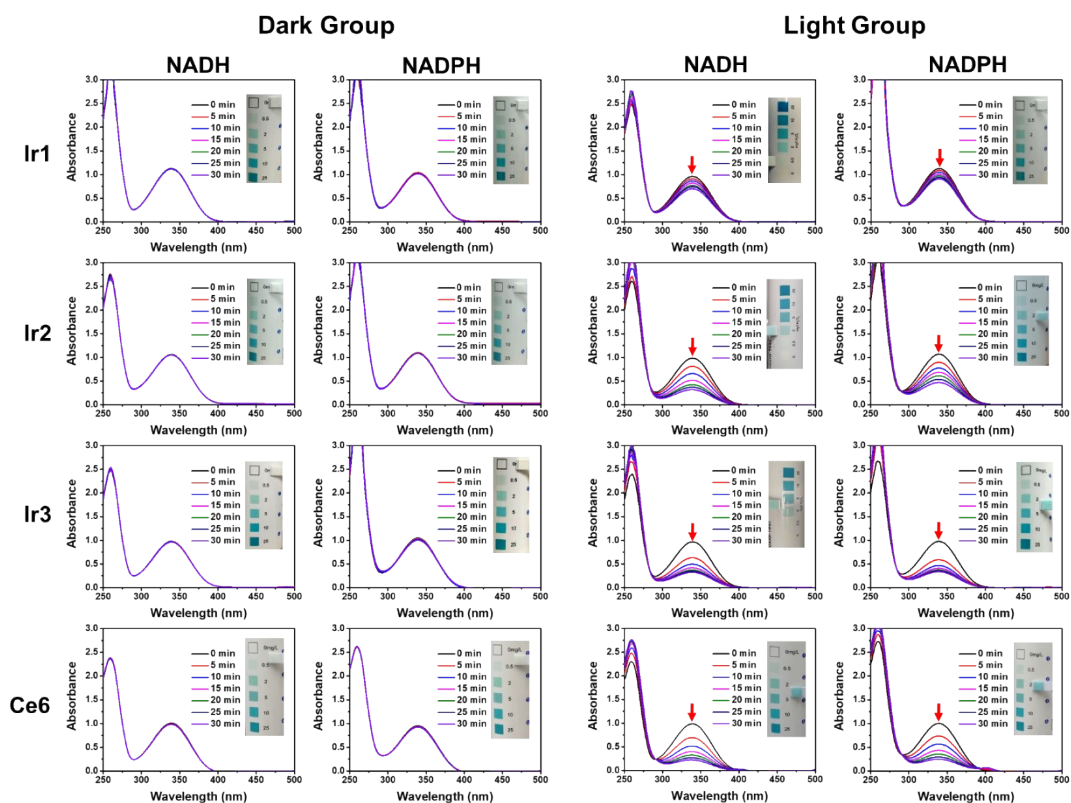


**Fig. S19.** UV-vis spectra showing the photocatalytic oxidation of NADH (160  $\mu\text{M}$ ) and NADPH (160  $\mu\text{M}$ ) by **Ir1** (5  $\mu\text{M}$ ), **Ir2** (5  $\mu\text{M}$ ), **Ir3** (0.5  $\mu\text{M}$ ) or Chlorin e6 (5  $\mu\text{M}$ ) in PBS. Insert:  $\text{H}_2\text{O}_2$  production after 30 min 465 nm light (power: 6.5  $\text{mW}/\text{cm}^2$ ) exposure. No significant NAD(P)H oxidation was observed in the dark.

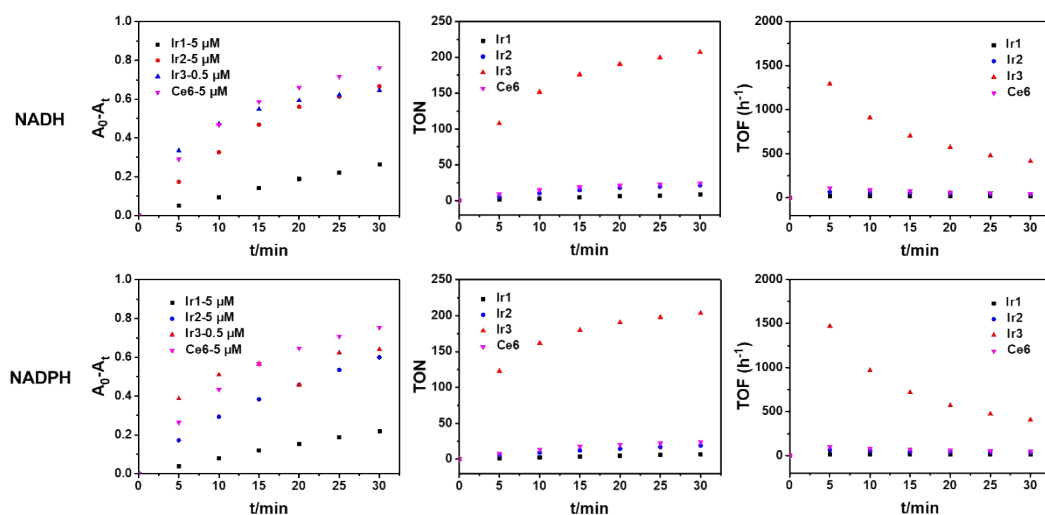


**Fig. S20.** Turnover number (TON) and turnover frequency (TOF) of **Ir1** (5  $\mu\text{M}$ ), **Ir2** (5  $\mu\text{M}$ ), **Ir3** (0.5  $\mu\text{M}$ ) and Chlorin e6 (5  $\mu\text{M}$ ) for NADH (160  $\mu\text{M}$ )/NADPH (160  $\mu\text{M}$ ) photo-oxidation after 30 min of light irradiation (monitored by UV-vis spectroscopy every 5 min).

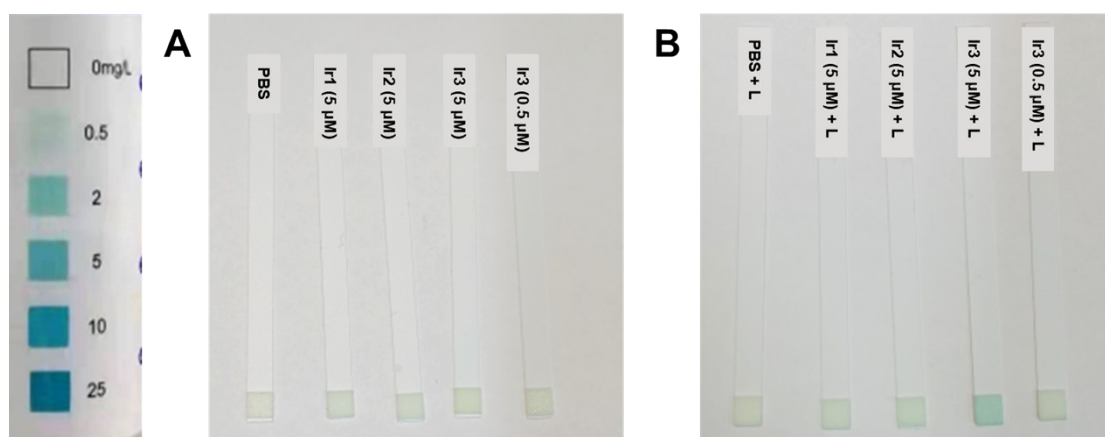


**Fig. S21.** Detection of  $\text{H}_2\text{O}_2$  in PBS solution produced by **Ir1** ( $5 \mu\text{M}$ ), **Ir2** ( $5 \mu\text{M}$ ), **Ir3** ( $0.5$  and  $5 \mu\text{M}$ ) after (A) dark and (B) light treatment ( $465 \text{ nm}$ ,  $11.7 \text{ J/cm}^2$ ) with NADH ( $160 \mu\text{M}$ ).

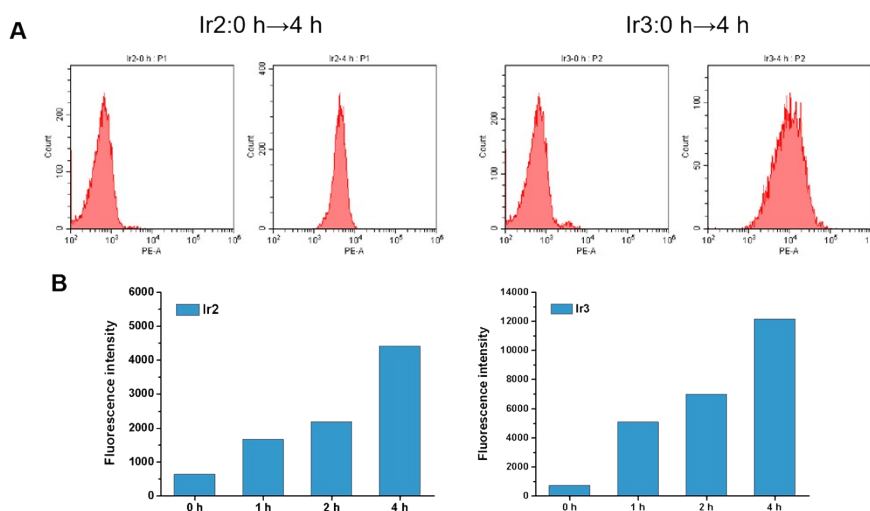


**Fig. S22.** (A) Time-dependent uptake of **Ir2** and **Ir3** in HeLa cells determined by measuring the intracellular emission intensity using flow cytometry. (B) Relative emission intensity of **Ir2** and **Ir3** in HeLa cells after treating with **Ir2** and **Ir3** (all  $10 \text{ M}$ ) for different incubation times ( $0 \text{ h}$ ,  $1 \text{ h}$ ,  $2 \text{ h}$  and  $4 \text{ h}$ ).



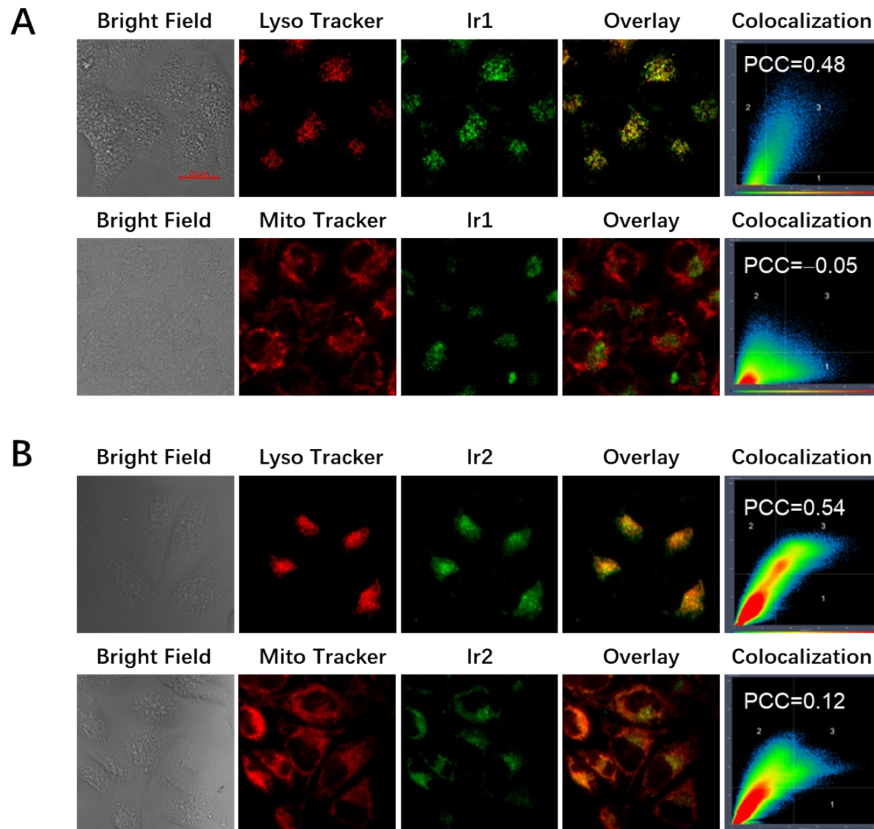


**Fig. S23.** Intracellular co-localization images in HeLa cells, incubated with (A) **Ir1** and (B) **Ir2** (all 10  $\mu$ M, 2 h) and LTDR (100 nM, 30 min) or MTR (100 nM, 30 min). **Ir1**:  $\lambda_{\text{ex}} = 405$  nm,  $\lambda_{\text{em}} = 500 \pm 40$  nm; **Ir2**:  $\lambda_{\text{ex}} = 458$  nm,  $\lambda_{\text{em}} = 540 \pm 40$  nm; LTDR:  $\lambda_{\text{ex}} = 633$  nm,  $\lambda_{\text{em}} = 680 \pm 20$  nm; MTR:  $\lambda_{\text{ex}} = 633$  nm,  $\lambda_{\text{em}} = 680 \pm 20$  nm. Scale bar = 20  $\mu$ m.

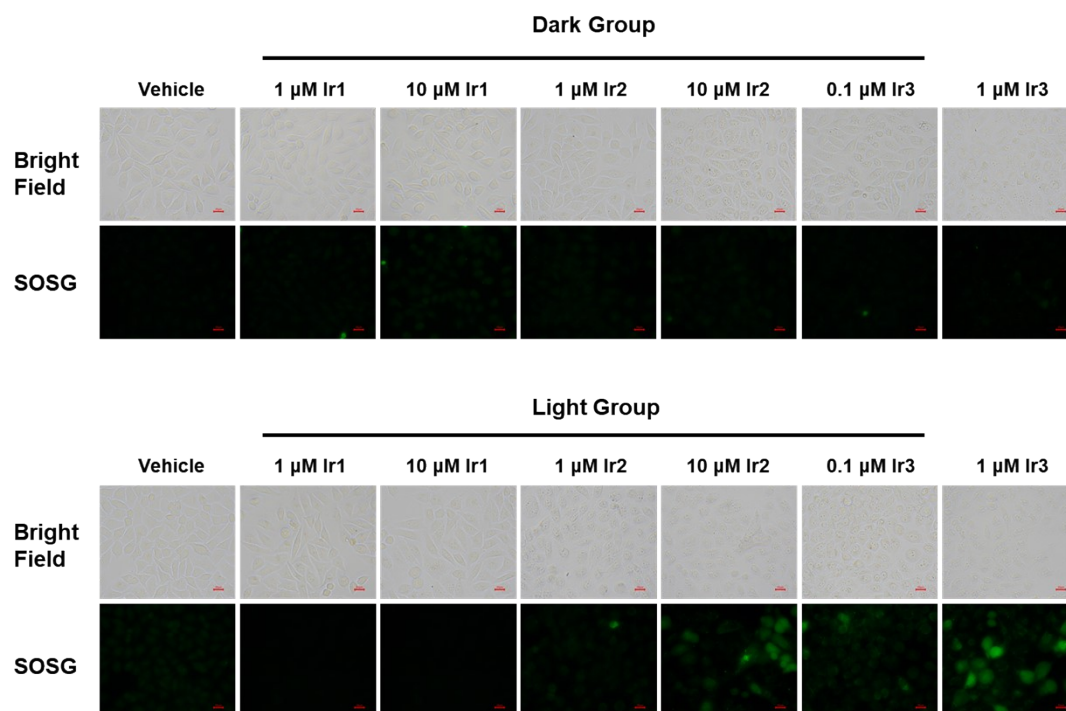


**Fig. S24.** Detection of intracellular singlet oxygen production in HeLa cells after treatment with **Ir1-Ir3**. SOSG was used as  $^1\text{O}_2$  fluorescence indicator. Cells were treated with **Ir1-Ir3** for 2 h in the dark, followed by incubation with singlet oxygen sensor green (SOSG) for 30 min after 5 min irradiation (465 nm, 39 mW/cm<sup>2</sup>, 5 min). The images were acquired by an inverted fluorescence microscope. Scale bar = 20  $\mu$ m.

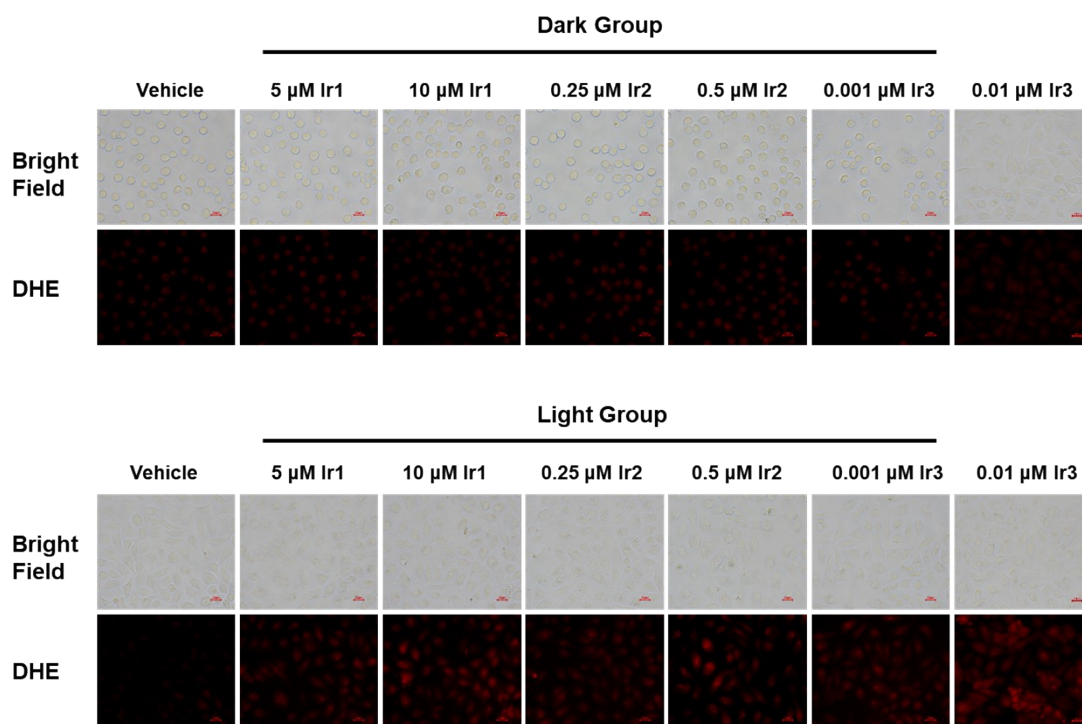


**Fig. S25.** Detection of superoxide radical anion production in HeLa cells after treatment with complexes **Ir1-Ir3**. Cells were incubated with **Ir1-Ir3** for 2 h in the dark, followed by 30 min incubation with dihydroethidium (DHE) after 5 min irradiation (465 nm, 39 mW/cm<sup>2</sup>, 5 min). The images were acquired using an inverted fluorescence microscope. Scale bar = 20  $\mu\text{m}$ .

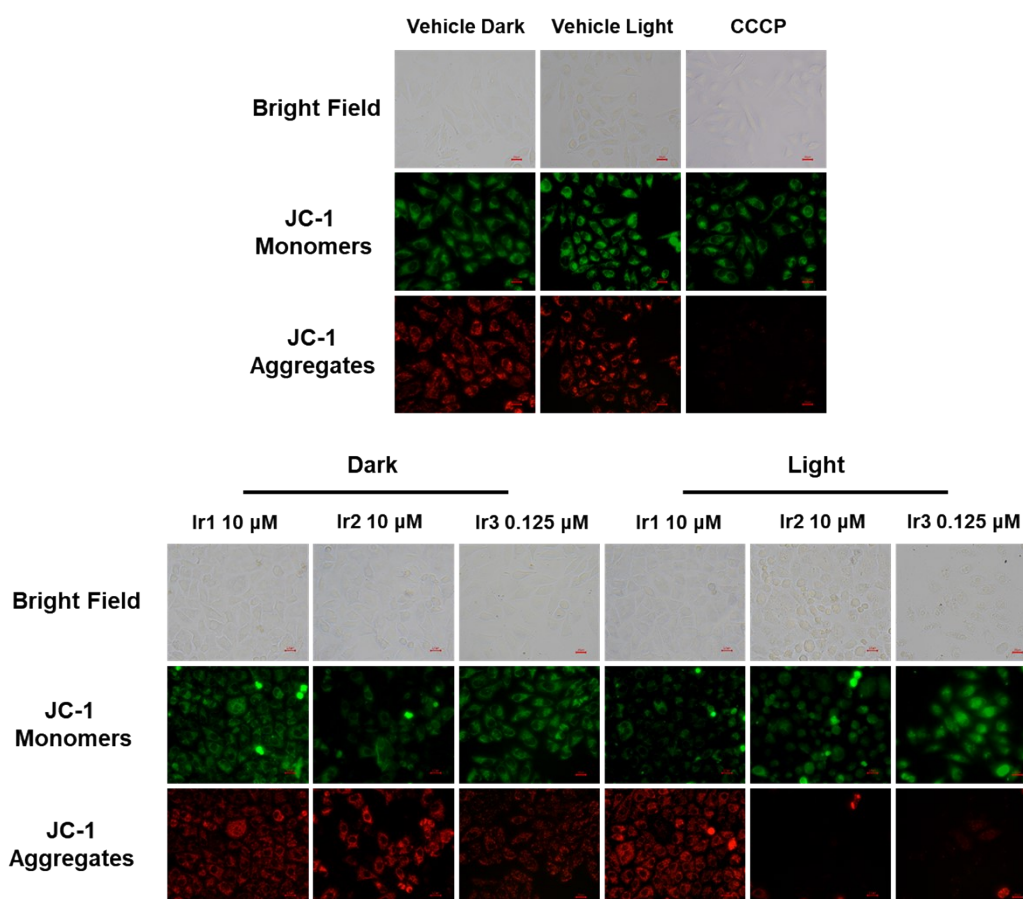


**Fig. S26.** JC-1 assay, showing the decrease in the mitochondrial membrane potential, induced by **Ir2**, **Ir3** and positive control drug CCCP on light irradiation. HeLa cells were treated with **Ir1** (10  $\mu$ M), **Ir2** (10  $\mu$ M) and **Ir3** (0.125  $\mu$ M) for 2 h or CCCP (50  $\mu$ M) for 5 min at 37  $^{\circ}$ C, followed by 5 min irradiation (465 nm, 39 mW/cm<sup>2</sup>, 5 min) and staining with JC-1 (2.5  $\mu$ g/mL, 20 min) respectively. Scale bar = 20  $\mu$ m.

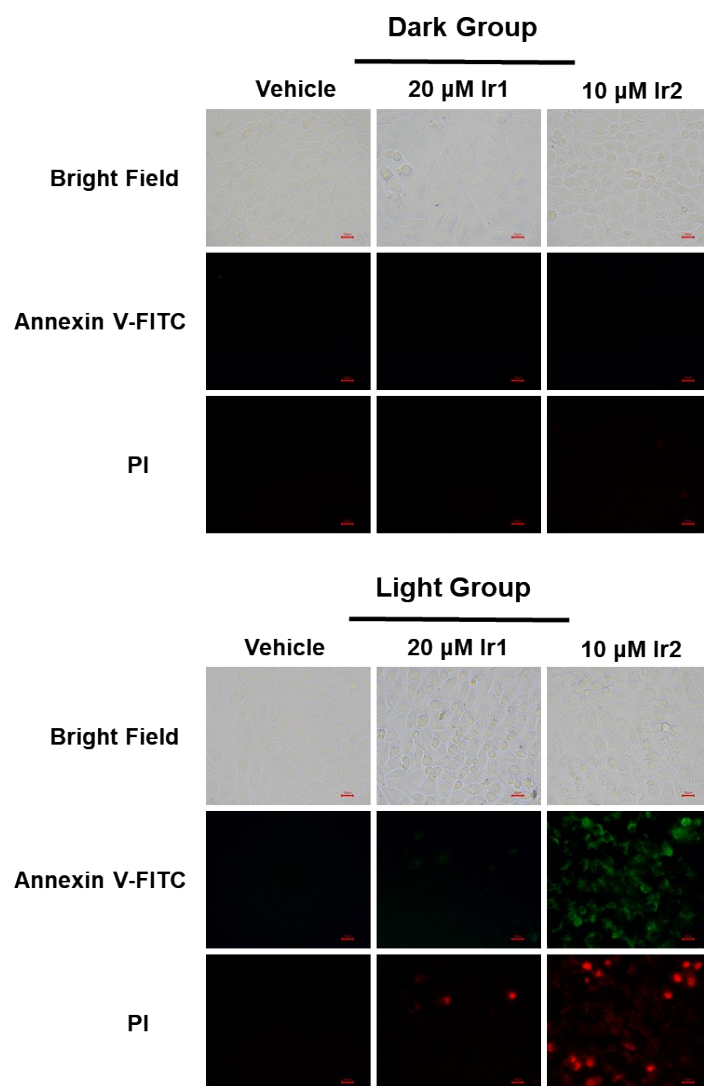


**Fig. S27.** Detection of the mode of HeLa cell death by Annexin V-FITC/PI staining after the treatment with **Ir1/Ir2** for 4 h. Cells were treated with various concentrations of **Ir1/Ir2** with or without light irradiation (465 nm, 39 mW/cm<sup>2</sup>, 5 min). Scale bar = 20  $\mu$ m.

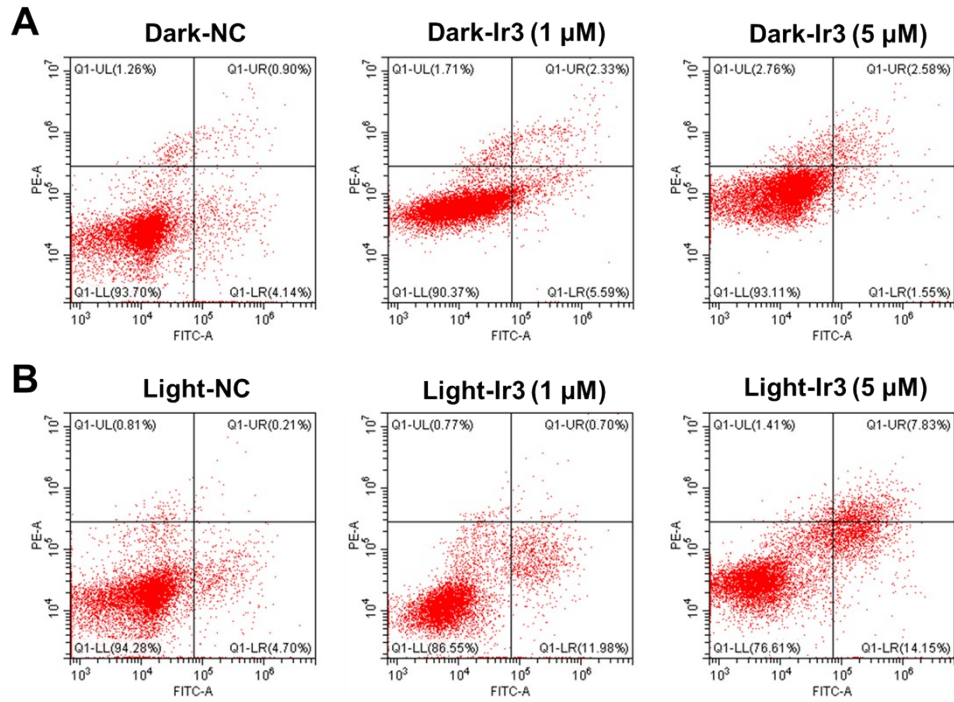


**Fig. S28.** Detection of the mode of Ir3-induced HeLa cell death by Annexin V-FITC/PI staining after the various treatments using flow cytometry. Cells were treated with various concentrations of Ir3 with or without light irradiation (465 nm, 39 mW/cm<sup>2</sup>, 5 min).

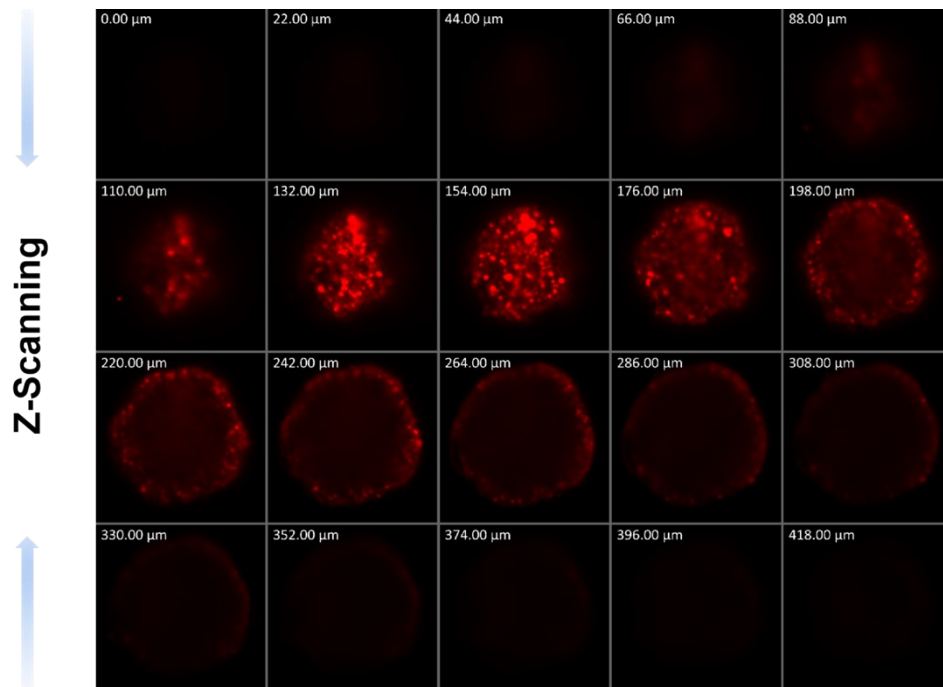


**Fig. S29.** Confocal Z-stack images of HeLa MCTs at 22  $\mu\text{m}$  intervals after incubating with Ir3 (5  $\mu\text{M}$ ) after 24 h. The images were obtained under a 20  $\times$  objective and excitation wavelength for imaging of 488 nm.

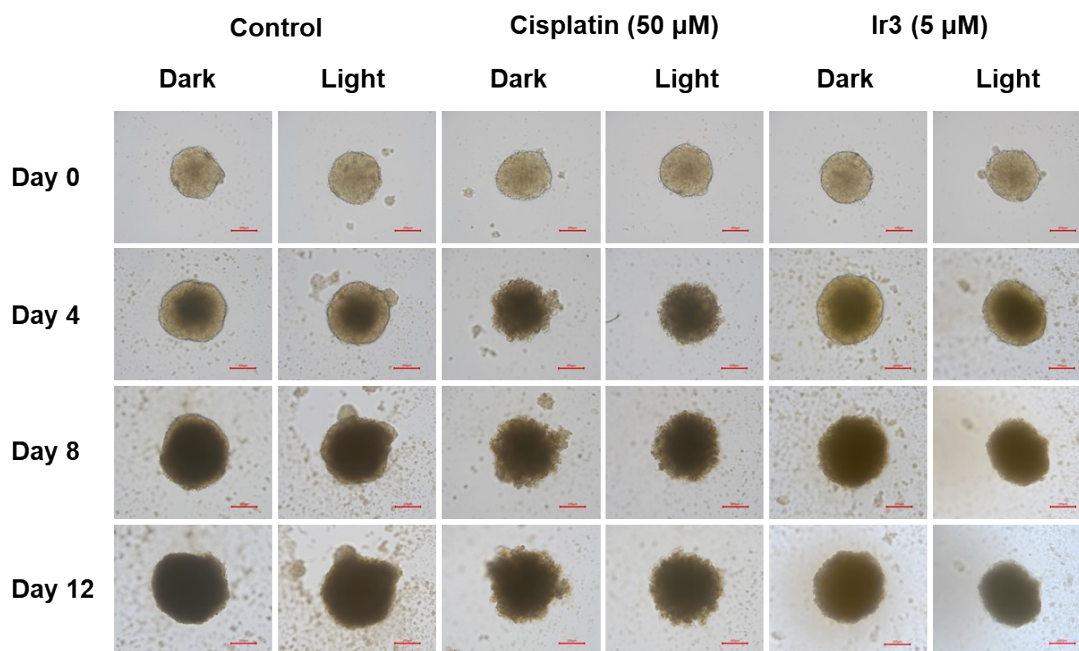


**Fig. S30.** Representative microscopic images of the growth inhibition of HeLa MCTSs after treatment with culture medium (control), cisplatin (50  $\mu$ M) and Ir3 (5  $\mu$ M) with or without light irradiation (465 nm, 39 mW/cm<sup>2</sup>, 5 min). The MCTSs were exposed to the indicated treatments for 24 h, followed by light irradiation on the first day. The images on Day 0 were recorded before the irradiation. After that the images were recorded every four days. Scale bar = 200  $\mu$ m.

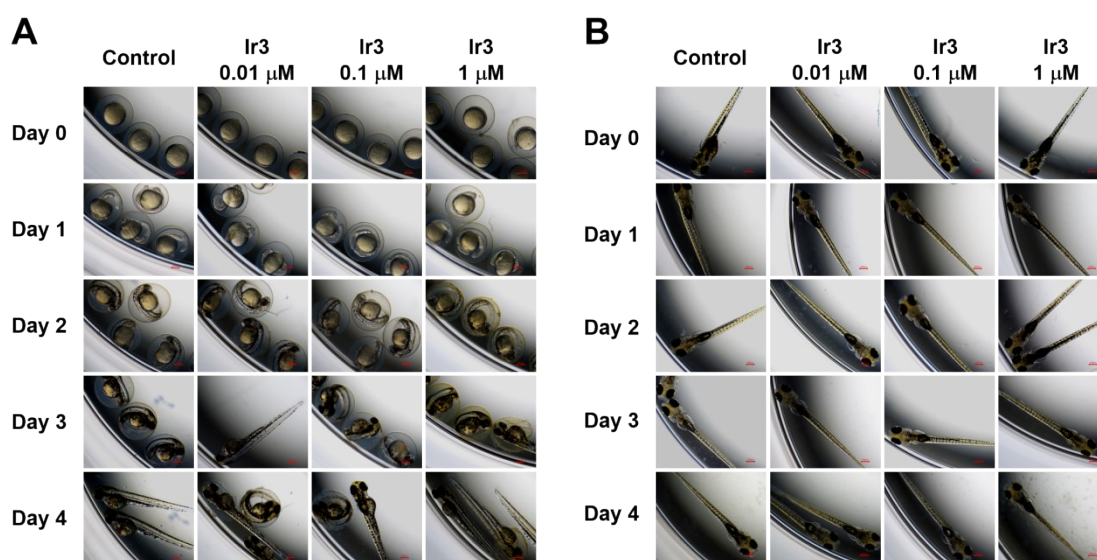


**Fig. S31.** Images for development and survival assay in (A) wild-type zebrafish embryos and (B) zebrafish larvae, after the treatment with Ir3 (0.01, 0.1 and 1  $\mu$ M) for 4 days (monitored by fluorescence microscopy every day). Scale bar = 200  $\mu$ m.

## References

- [1] C. Huang, C. Liang, T. Sadhukhan, S. Banerjee, Z. Fan, T. Li, Z. Zhu, P. Zhang, K. Raghavachari, H. Huang, *Angew. Chem. Int. Ed.*, 2021, **60**, 9474-9479.
- [2] H. Ishidaa, S. Tobitab, Y. Hasegawac, R. Katohd, K. Nozakie, *Coord. Chem. Rev.*, 2010, **254**, 2449-2458.
- [3] C. Lia, Y. Wang, Y. Lu, J. Guo, C. Zhu, H. He, X. Duan, Mei Pan, C. Su, *Chin. Chem. Lett.*, 2020, **31**, 1183-1187.
- [4] H. Huang, S. Banerjee, K. Qiu, P. Zhang, O. Blacque, T. Malcomson, M. J. Paterson, G. J. Clarkson, M. Staniforth, V. G. Stavros, G. Gasser, H. Chao, P. J. Sadler, *Nat. Chem.*, 2019, **11**, 1041-1048.
- [5] Z. Zhou, J. Liu, J. Huang, T. W. Rees, Y. Wang, H. Wang, X. Li, H. Chao, P. J. Stang, *Proc. Natl. Acad. Sci. U. S. A.*, 2019, **116**, 20296-20302.
- [6] S. Jin, D. Beis, T. Mitchel, J. Chen, D. Y. R. Stainier. *Development*, 2005, **132**, 5199-5209.
- [7] J. P. C. Coverdale, H. E. Bridgewater, J. Song, N. A. Smith, N. P. E. Barry, I. Bagley, P. J. Sadler, I. Romero-Canelón, *J. Med. Chem.*, 2018, **61**, 9246-9255.